

TECTONO-STRATIGRAPHIC EVOLUTION OF THE AYHAN BASIN,
CENTRAL ANATOLIA, TURKEY: A LATE CRETACEOUS TO EARLY-
EOCENE SUPRA DETACHMENT BASIN THAT UNDERWENT POST-
LUTETIAN COMPRESSION AND TILTING

Advokaat, E.L.



TECTONO-STRATIGRAPHIC EVOLUTION OF THE AYHAN BASIN, CENTRAL ANATOLIA, TURKEY: A LATE CRETACEOUS TO EARLY- EOCENE SUPRA DETACHMENT BASIN THAT UNDERWENT POST- LUTETIAN COMPRESSION AND TILTING

Advokaat, E.L.

ABSTRACT

The Ayhan basin is located in the center of the Central Anatolian Crystalline Complex (CACC). Adjacent to the Ayhan basin are the metamorphic blocks of Hırkadağ to the west and İdis Dağı to the east. These expose Cretaceous metamorphic rocks of amphibolite to upper amphibolite facies which are intruded by granites and syenitoids with an assumed Maastrichtian age.

The formation of the Ayhan Basin was caused by N-S directed extensional faulting, evidenced by the steep N-dipping normal fault which forms the southern boundary of the basin. This fault was activated during emplacement of the Karahidir volcanics in the Campanian-Maastrichtian. These volcanics are reworked throughout the complete sedimentary sequence of the Ayhan basin.

The history of the Ayhan Basin is characterised by pre-Lutetian syn-sedimentary extension, evidenced by syn-sedimentary normal faults. During this extension the basin is dominated by continental sediments associated with fluvial and lacustrine paleo-environments. Only during the Lutetian, marine nummulitic limestones are deposited. N-S directed compression started after the Lutetian. During this compression the basin is deformed by folds and south dipping thrust faults. The volcanics at the southern boundary are thrust northwards over the sedimentary sequence. After this compression the basin is tilted and uplifted. Northernly dipping clastic sediments are deposited, which unconformably overlie the Campanian – Lutetian sediments. The post-Lutetian sediments are covered by the volcanic tuffs of the Ürgüp Formation. After the stage of tilting, the metamorphic Hırkadağ and İdis Dağı Block are uplifted by steeply dipping normal faults.

Based on detailed mapping of the Ayhan Basin, balanced cross-sections are created. Restoration of these cross-sections quantify a shortening of ~2 km.

Exhumation of the Hırkadağ Block is accommodated by a low angle detachment fault. Unroofing of the Hırkadağ and İdis Dağı blocks is only recorded in the Upper Group of the sedimentary sequence of the Ayhan Basin. At the base of this Upper Group metamorphic detritus is found. Therefore, in the study area, the unroofing of the surrounding metamorphic blocks can only be dated to be post-Lutetian. This is opposed to the regional geology of the CACC, where unroofing is pre-Eocene, indicated by middle-Eocene deposits which unconformably overlie the metamorphic rocks of the CACC.

CONTENTS

<u>ABSTRACT</u>	<u>1</u>
<u>CONTENTS</u>	<u>2</u>
<u>1. INTRODUCTION</u>	<u>3</u>
<u>2. GEOLOGICAL SETTING</u>	<u>5</u>
<u>3. LITHOLOGY</u>	<u>8</u>
METAMORPHIC AND IGNEOUS BASEMENT	8
STRATIGRAPHY OF THE SEDIMENTARY COVER	10
AGE OF SEDIMENTS	16
<u>4. STRUCTURE</u>	<u>16</u>
NORTHERN PART	16
WESTERN PART	21
CENTRAL PART	23
EASTERN PART	24
<u>5. DISCUSSION</u>	<u>24</u>
GEOLOGICAL HISTORY	24
PALEOGEOGRAPHIC STRUCTURE	26
TIMING OF TECTONIC EVENTS	27
<u>6. CONCLUSIONS</u>	<u>28</u>
<u>7. ACKNOWLEDGEMENTS</u>	<u>28</u>
<u>8. REFERENCES</u>	<u>29</u>
<u>9. APPENDICES</u>	<u>30</u>

1. INTRODUCTION

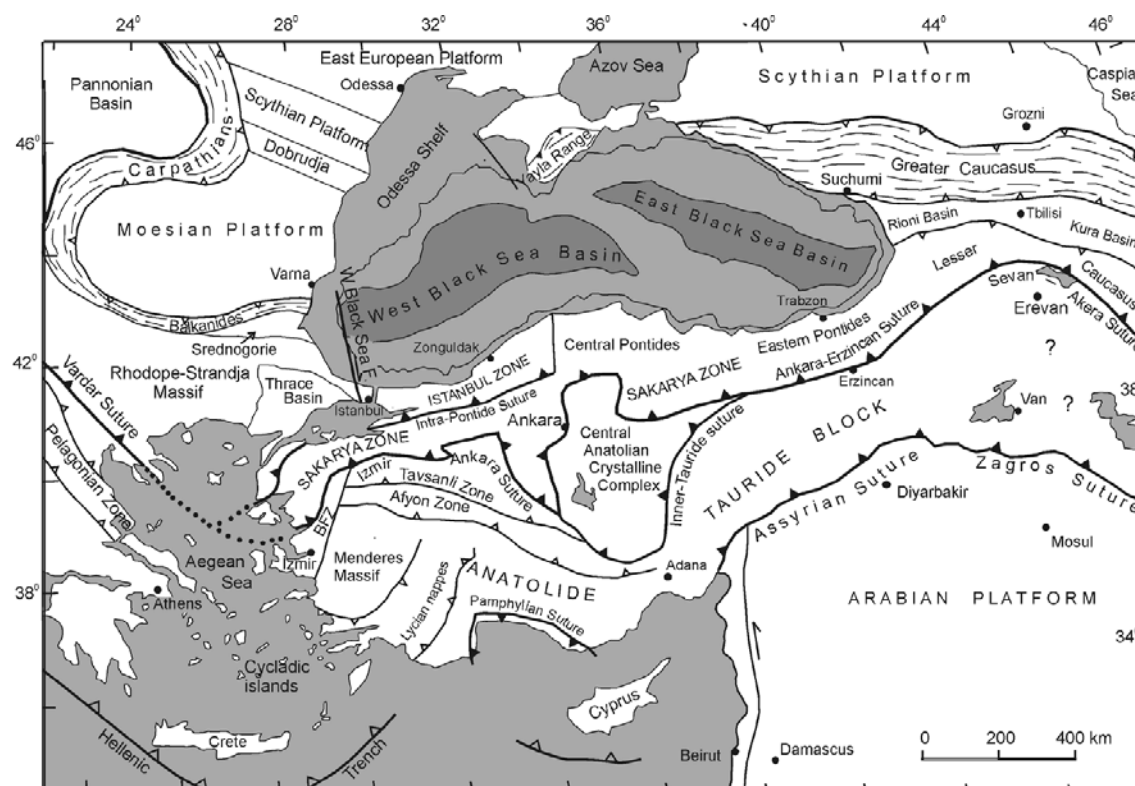


Figure 1. Tectonic map of Turkey and surrounding regions showing the major sutures and continental blocks. Sutures are shown by heavy lines with the polarity of former subduction zones indicated by filled triangles. Heavy lines with open triangles represent active subduction zones. Small open triangles indicate the vergence of the major fold and thrust belts. BFZ denotes the Bornova Flysch Zone (Okay, 2008, modified after Okay & Tüysüz, 1999).

Turkey is characterized by a very complex geology comprising several continental blocks, separated by suture zones (see figure 1).

The Pontides in the N, and the Sakarya Continent (regarded as sub-massif of the Pontides by some authors (Okay, 2008; Kaymakci et al., 2009) and by others (Şengör & Yılmaz, 1981) as an independent continental fragment) in the NW. The northern massifs (Strandja, Istanbul, Sakarya), often generalised as the Pontides, all show a Variscan phase of deformation and metamorphism. The Pontides are interpreted as a magmatic arc with Laurasian affinity, being the result of the northward subducting Neo-Thetys Ocean. The Black Sea is regarded as a back-arc extensional basin, which formed during the Cretaceous (Okay, 2008). The southern boundary of the Pontides (and Sakarya continent) is marked by the Izmir-Ankara-Erzincan Suture Zone (IEAS Zone).

The Anatolides-Taurides comprise most of South Anatolia (Bornova Flysch Zone, Tavşanlı Zone, Menderes Massif & Afyon Zone and the Taurides). The Anatolides-Taurides formed the former northern passive margin of Gondwanaland (Şengör & Yılmaz, 1981; Okay, 2008). The Afyon Zone, which forms the boundary with the CACC, is a blueschist belt of Cretaceous age, with metamorphic peak conditions showing HP/LT metamorphism that were reached around 60Ma (Şengör & Yılmaz, 1981; Pourceau et al., 2010; Okay, 2008).

The Central Anatolian Crystalline Complex (CACC) is located between the Pontides and the Anatolides-Taurides. The southern boundary of the CACC with the Anatolides-Taurides is formed by the Inner-Tauride High Pressure belt (the Afyon Zone). Within the literature, there is no general agreement on the origin of the CACC. Some authors (Göncüoğlu et al., 1997; Floyd et al., 2000) argue that the CACC forms the northern margin of the Anatolides-Taurides, since they state that:

1.) No ophiolitic belt is exposed between the Anatolides-Taurides and the CACC.
 2.) There are great lithostratigraphic similarities between the two blocks.
 Others, (*Pourteau et al., 2010*) consider the CACC as a separate continental fragment. This is mainly based on the following argument (*Pourteau et al., 2010* and *references therein*):

- 1.) The Lycian, Kütahta and Tauride ophiolites are from one oceanic basin, evidenced by the metamorphic sole ages which are all around 100-90 Ma and comparable lithologic and geochemical features. However, the ophiolites lying on top of the CACC differ from the Lycian, Kütahta and Tauride ophiolites by their lithostratigraphy.
- 2.) Furthermore, no high-pressure (HP) material has ever been reported for the Central Anatolian Ophiolites. Based on these arguments, this group of authors argued that Lycian, Kütahta and Tauride ophiolites on one hand and the Central Anatolian Ophiolites on the other are derived from two separate oceanic branches.

Additionally *Pourteau et al. (2010)* showed with tectonic reconstructions, based on paleomagnetic data, that the Anatolides-Taurides have been bended around the southern tip of the CACC during the Eocene.

Both the S-side of the Sakarya continent and the N-side of the CACC were passive margins with an oceanic plate attached. Intra-oceanic N-wards subduction of the CACC oceanic plate under the Sakarya oceanic plate resulted in obduction of the overriding Sakarya oceanic plate during the Early Cretaceous to Santonian (*Sengör & Yilmaz, 1981; Kaymakci et al., 2009*). After this obduction, collision of the two continental blocks occurred during the Campanian to Paleocene (*Sengör & Yilmaz, 1981; Kaymakci et al., 2009*).

The CACC is composed of metasedimentary rocks. The structurally lowest units are presumably of Late Paleozoic age (Silurian-Devonian), while the upper units, dominated by marbles, are of Triassic to Early Cretaceous age (*Floyd et al., 2000*). Radiometric dating of the metamorphic rocks of the Niğde dome in the south of the CACC by *Whitney et al. (2003)* determined that metamorphic peak conditions of LP/HT metamorphism were reached at 91.0 ± 2.0 Ma.

The metamorphic rocks of the CACC are intruded by granitoids and syenitoids. Based on Zircon ^{207}Pb - ^{206}Pb evaporation ages, *Boztug et al. (2009a)* defined three clusters of intrusions: (1) Cenomanian-Turonian (94.9 ± 3.4 Ma), (2) Turonian-Santonian (85.5 ± 5.5 Ma) and (3) Campanian (74.9 ± 3.8 Ma). These granites were rapidly exhumed during the Campanian to Maastrichtian (80 - 65 Ma), which is based on ^{40}Ar - ^{39}Ar and ^{40}K - ^{40}Ar cooling ages (*Boztug et al., 2009a*). Apatite fission track ages mark the end of exhumation at 62-57 Ma (*Boztug & Jonckheere, 2007*). The age of exhumation of metamorphic and intrusive rocks of the CACC is well dated, but the mechanisms by which they are exhumed are poorly constrained.

Volcanics overlying the metamorphic and granitoid rocks are cogenetic with the late stage syenitoid intrusions (*Köksal & Göncüoğlu, 2001*). These volcanics are assumed to be of Pre-Maastrichtian – Paleocene age (*Göncüoğlu et al., 1993*) and have an andesitic composition. These volcanics have overlain large areas of the CACC, but only isolated outcrops in the NW, NE and the central part of the CACC remain (*Gökten & Floyd, 1987; Kara & Dönmez, 1990; Şenel, 2002*).

The CACC is unconformably covered by sedimentary rocks of Eocene age (*Şenel, 2002*). Within the CACC, there are some basins around the Kaman region (*Norman et al., 1980*) and the central part of the CACC – the Hırkadağ and İdis Dağı regions – where also sediments from pre-Eocene age are reported (*Atabey, 1989; Teklehaimanot, 1993; Göncüoğlu, 1993; Köksal & Göncüoğlu, 1997*).

The aim of this study is to investigate whether these Pre-Eocene sediments unconformably cover the basement units or record the (syn-)exhumation history of the CACC. Therefore, the Ayhan Basin in the central part of the CACC is investigated.

This study will focus on:

1. The structure of the deformed sedimentary sequence
2. The balancing of the structural cross-section to determine the pre-folding and thrusting geometry & to determine the amount & percentage of shortening.
3. The characterization of the sedimentary history of the basin.
4. Possibly age dating of the basin by use of palynology and radiometric ^{40}K - ^{40}Ar dating.

In this paper we present a revised detailed map of the Ayhan Basin, balanced cross sections of the deformed basin and the results of the analysis of the sedimentary history of the basin.

2. GEOLOGICAL SETTING

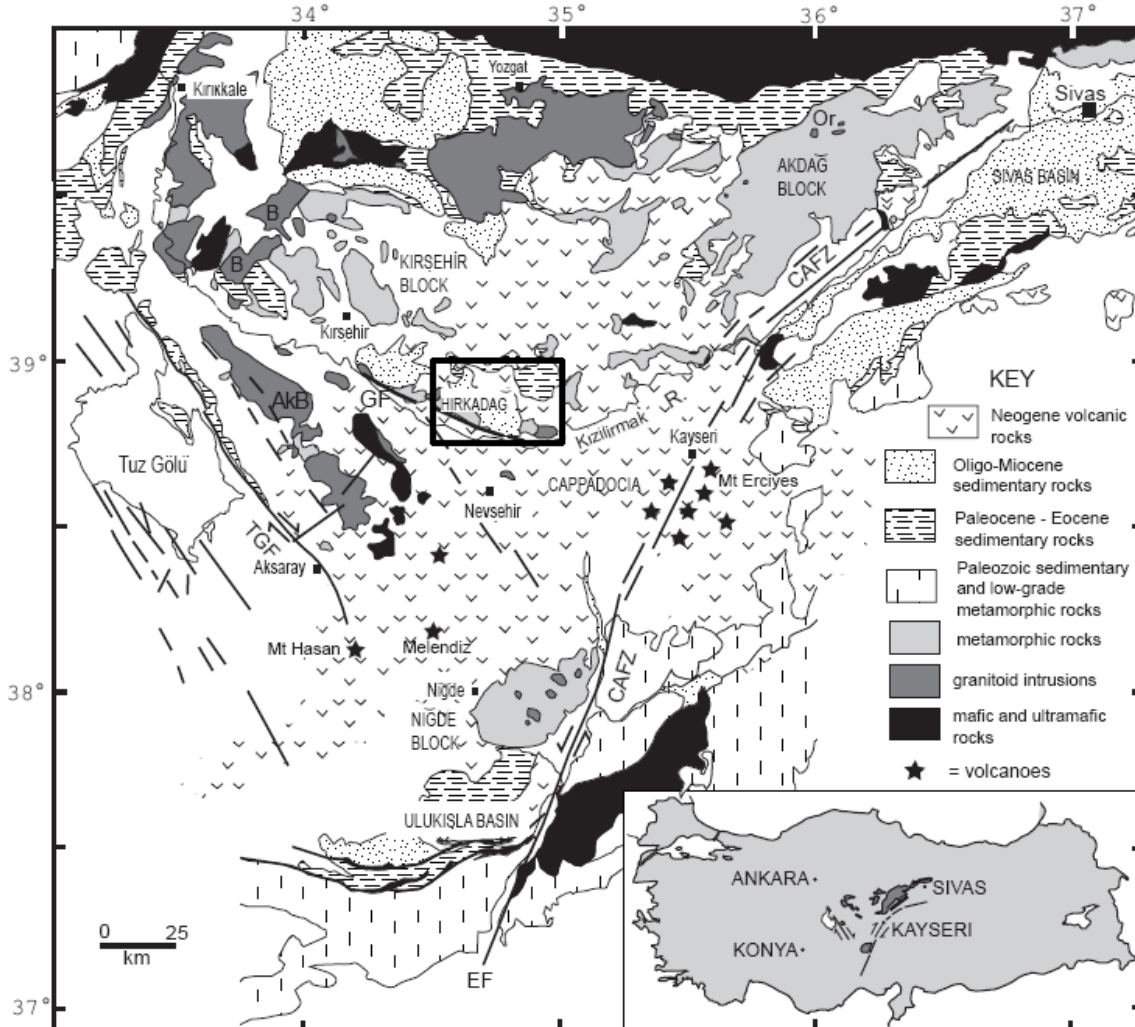


Figure 2. Geologic map of the Central Anatolian Crystalline Complex and vicinity, from Whitney and Dilek (2001). Inset: Map showing the location of the CACC in central Turkey. Area in box: Hırkadağ, Ayhan and İdis Dağı region (see figure 4.) Key to abbreviations: AkB- Aksaray block; B- Baranadağ pluton; CAFZ- Central Anatolian fault zone; EF- Ecemiş segment of the CAFZ (extends to Kayseri region); GF- Gümüşkent fault; Or- Ortaköy pluton; TGF- Tuz Gölü fault.

The Central Anatolian Crystalline Complex (CACC) is a triangular metamorphic complex, comprising three sub-massifs: in the NE the Akdağ Massif, in the S the Niğde Massif and in the NW the Kırşehir Massif. The study area is located in the Kırşehir Massif, 20 km north of Nevşehir (see figure 2). The lithology of the Central Anatolian Metamorphics comprises three units (Göncüoğlu et al, 1991; Floyd et al, 2000; Whitney et al, 2001; Gautier et al., 2008). (1) The structurally lowest formation of Paleozoic age is dominated by high grade (upper

amphibolite facies) marbles, calc-silicates amphibolite, gneiss and quartzites. (2) The overlying Mesozoic unit consists of lower grade (amphibolite facies) marbles, calc-silicates, mica schists and amphibolites. (3) The structurally highest unit of Mesozoic age consists of lowest grade (greenschist to lower amphibolite facies) coarse grained marble, calc-silicate, quartzite, mica schist, meta-peridotite. Ophiolitic fragments (pillow lavas, dykes, ultramafic gabbros) are overlying the metamorphics (see figure 3a)

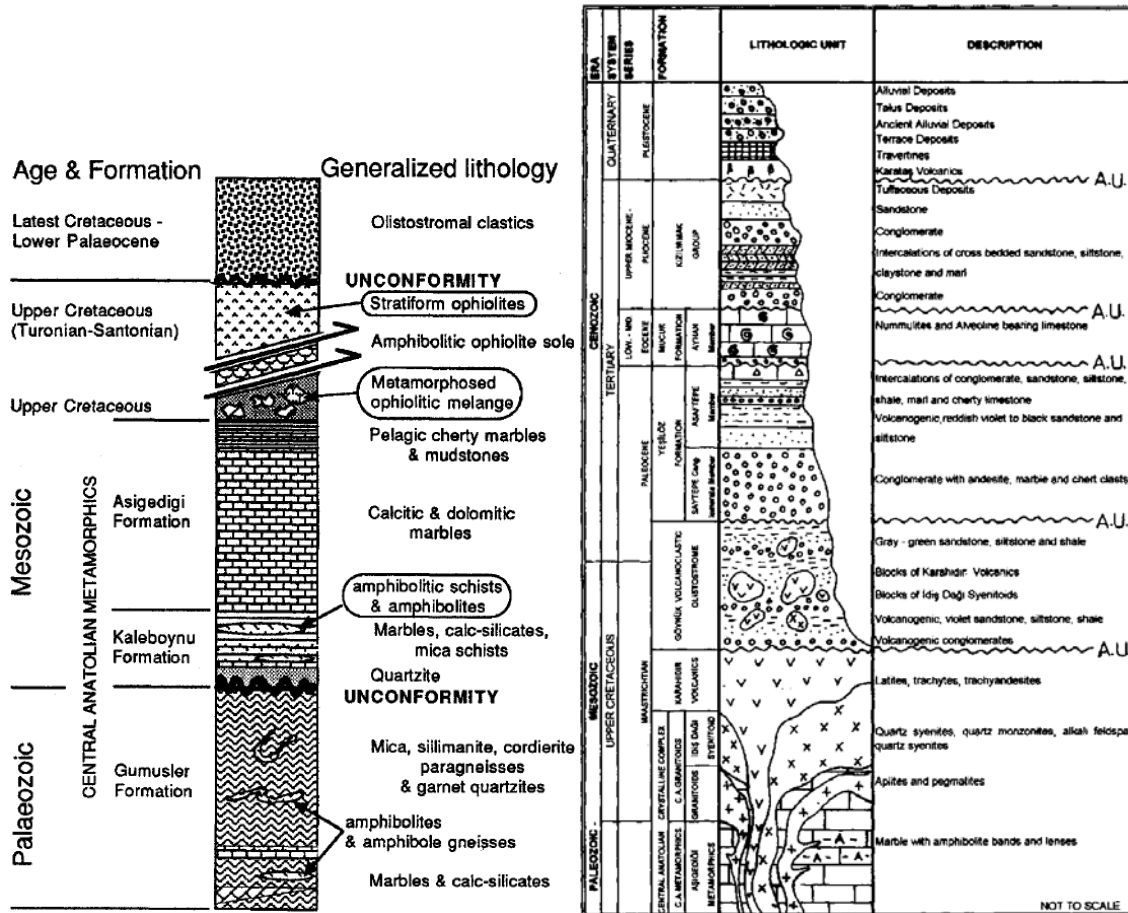


Figure 3. (a) Left: Generalised stratigraphic column (not to scale) for the CACC (Göncüoğlu et al., 1991) (b) Right: Stratigraphic column (not to scale) for the İdis Dağı area (Köksal et al., 1997). Note the volcanics that cover the metamorphic and igneous basement.

The metamorphic rocks of the Hırkadağ block consist of metapelites, quartzites and marbles of high grade amphibolite facies (Teklehaimanot, 1993; Wehrens, 2008). The metamorphic rocks in the İdis Dağı block consist of marbles, amphibolites and amphibolite schists of medium to high grade amphibolite facies (Köksal & Göncüoğlu, 1997).

The massifs are intruded by granites and syenitoids and overlain by volcanics. In the study area the metamorphic blocks (Hırkadağ and İdis Dağı) are intruded by granitoids and the İdis Dağı Syenitoids. In the study area, volcanics are found at the southern and western boundary of the Ayhan Basin. These are identified as the Karahidir volcanics, which are cogenetic with the İdis Dağı Syenitoids, and have overlain the metamorphic blocks in some regions of the CACC (Gökten & Floyd, 1987; Kara & Dönmez, 1990; Şenel, 2002). These volcanics are assumed to be of pre-Maastrichtian to Paleocene age (Göncüoğlu et al., 1993) and have an andesitic composition. Petrographic and geochemical data of the syenitoids and these volcanics show similar patterns, indicated to be typical of post-collisional, A-type igneous rocks (Köksal et al., 2001).

The western boundary of the Ayhan Basin is a steep ENE dipping normal fault which juxtaposes the basin to the metamorphic Hirkadağ block (Whitney & Dilek, 2001). The eastern boundary is a steep SSE dipping thrust fault (Köksal & Göncüoğlu, 1997; Köksal et al., 2001), which puts the İdis Dağı block, in contact with the Ayhan basin. To the southwest, the basin is bounded by volcanics and granitoids. The northern boundary of the basin is formed by Miocene (Tortonian) volcanic tuff, commonly referred to as the Ürgüp Fm (Atabey, 1989; Mues-Schumacher and Schumacher, 1996; Viereck-Goette et al., 2010), which overly the upper strata of the basin.

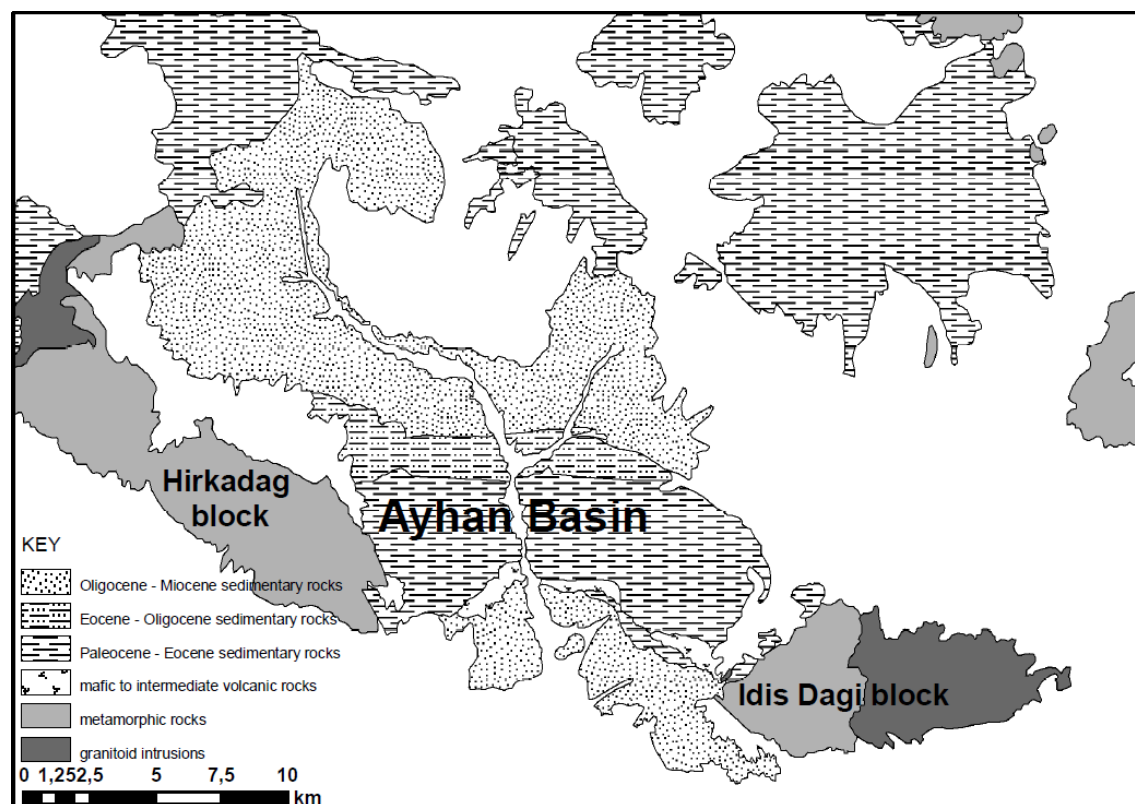


Figure 4. Simplified geological map (contours after Atabey, 1989) of the study area showing the Ayhan Basin surrounded by the Hirkadağ block at the west, the İdis Dağı block at the east and volcanics to the south.

3. LITHOLOGY

METAMORPHIC AND IGNEOUS BASEMENT

(BM) Basement: Metamorphics

The sedimentary rocks of the Ayhan Basin are surrounded by metamorphic and igneous basement. The metamorphic rocks in the İdis Dağı block consist of marbles, amphibolites and amphibolite schists in medium to high grade amphibolite facies (Köksal & Göncüoğlu, 1997). The metamorphic rocks of the Hırkadağ block consist of metapelites, quartzites and marbles in high grade amphibolite facies (Teklehaımanot, 1993, Wehrens, 2008).

(BI) Basement: Intrusives

The metamorphic Hırkadağ and İdis Dağı blocks are intruded by granitoids (Teklehaımanot, 1993) and syenitoids (Göncüoğlu, 1993; Köksal & Göncüoğlu, 1997; Köksal et al., 2001). The pluton in the Hırkadağ block is determined as granitic to granodioritic (Teklehaımanot, 1993, Whitney & Dilek, 2001), composed of alkali feldspars, plagioclase and quartz as major constituents and amphiboles as minor constituent (Teklehaımanot, 1993).

The İdis Dağı pluton is defined as syenitoid, because of the low amounts of quartz. The rocks are characterized by large (up to 3 cm) alkali feldspar crystals with well developed tabular appearance. In minor amounts and smaller grain size quartz, plagioclase and biotite minerals are present (Köksal & Göncüoğlu, 1997).

The intrusive bodies in the study area have not been radiometrically dated, but ages are inferred from other intrusive bodies in the CACC and are assumed to be Late Cretaceous. Both the Hırkadağ and İdis Dağı block contain intrusive bodies. At the southern boundary of the basin intrusive rocks occur. In the southwest they are thrust over the sedimentary sequence along with the volcanics. In the southeastern part they are in contact with volcanics and sediments by a N-dipping normal fault. To the south, this intrusive body is overlain by conglomerates (see figure 5).

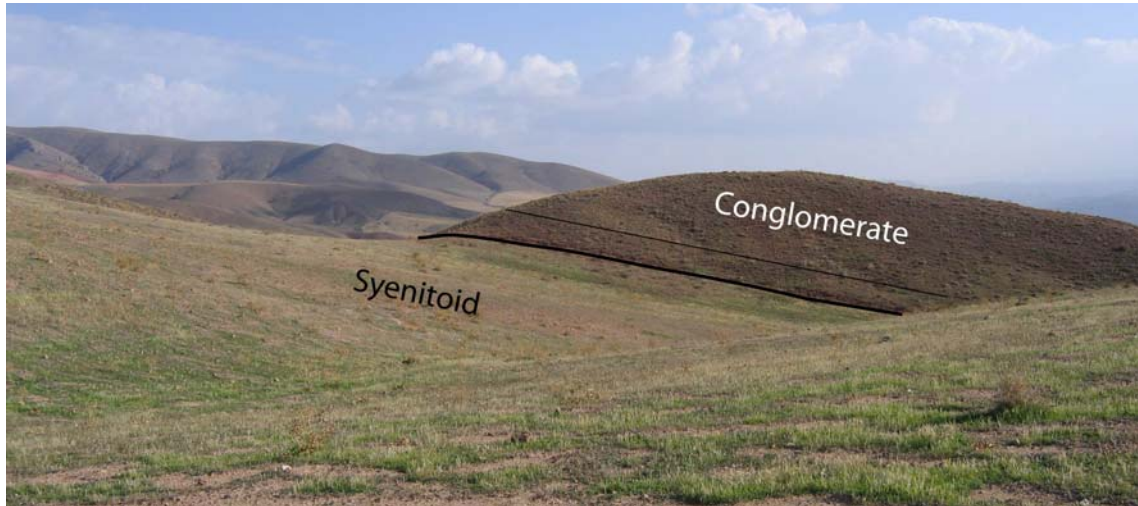
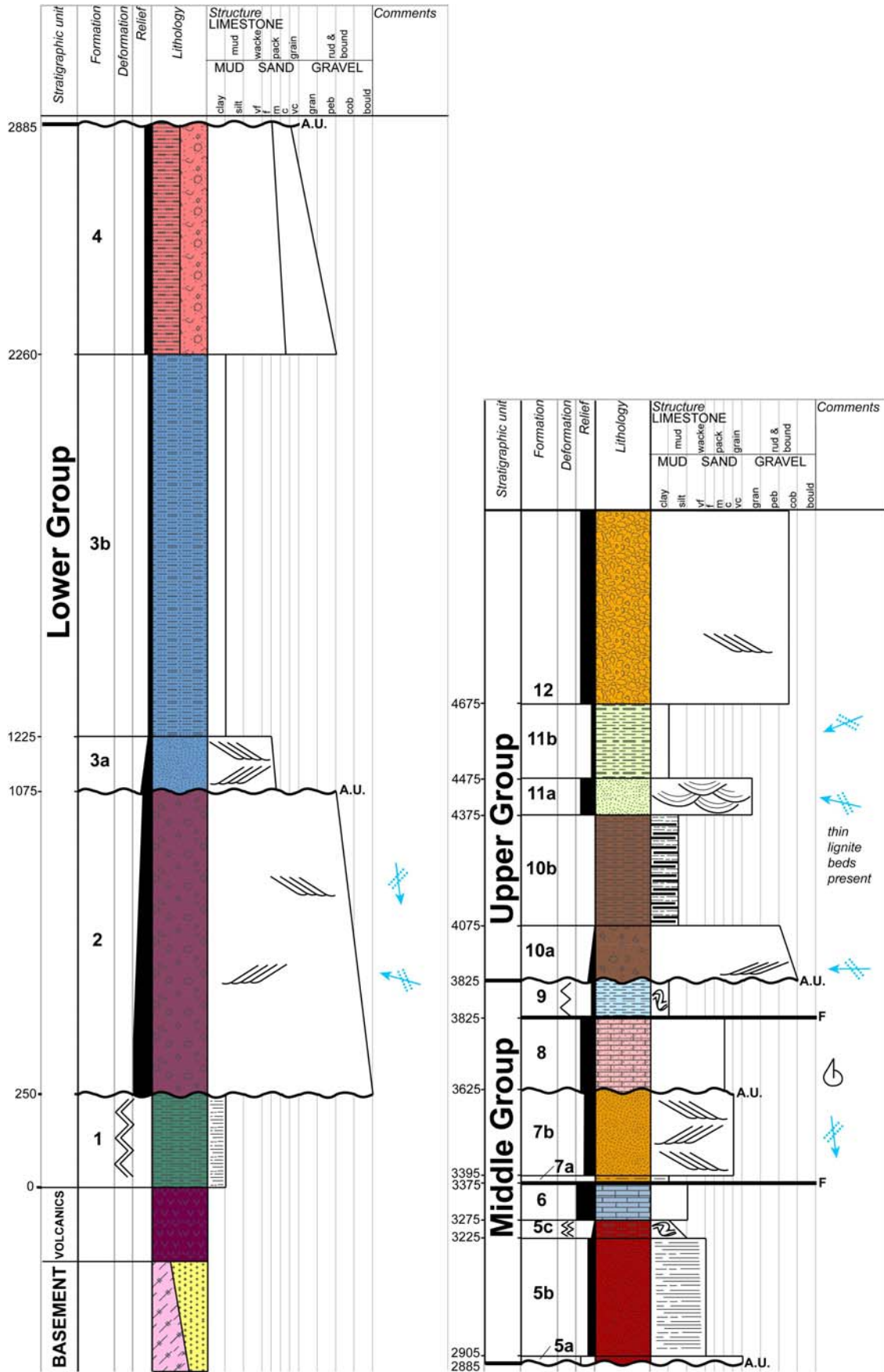


Figure 5. Syenitoid covered by S-dipping conglomerate. View of photograph to east

Figure 6. (following page) Composite stratigraphic column of the Ayhan Basin. For stratigraphic thickness, maximum thicknesses are used. Basement units and volcanics are not to scale. Key is same as for the Geological map (Appendix 1). Note the similarity with the stratigraphy of the İdis Dağı region (see figure 3b.)



STRATIGRAPHY OF THE SEDIMENTARY COVER

On basis of geometrical and structural relationships, the lithology of the basin can be divided in three mappable groups of formations. The Lower Group (Fm 1-4) is exposed in a large-scale monoclinical structure, which forms the western part of the basin. The Middle Group (Fm 5-9) is affected by an east-west trending fold-and-thrust system in the centre of the exposed part of the basin. In the northern part of the basin, the Upper Group (Fm 10-12) unconformably overlies both earlier groups and their structures, with a northerly dip of ~ 20-30°.

The present day exposure of the basin is only a partial one. The basin is bounded both at the west and east by high angle faults, where metamorphic rocks are juxtaposed to sedimentary rocks. This indicates that the basin extended more towards the west and east. The northern part of the basin is covered by N-dipping sediments which obscure the most northern extent of the basin. The bounding normal fault at the southern edge of the basin is probably the former basin extent. The base of the sedimentary sequence is formed by volcanics.

KV: Karahidir Volcanics

The basement rocks are overlain by volcanic rocks, which are trachytic, latitic and andesitic types (Köksal *et al.*, 2001). These form the floor of the basin. This is observed in the very west part of the basin near the normal fault contact with the metamorphic basement, where the violet conglomerate (Fm1) lies on top of the volcanics. At the west bank of the Kızılöz river, intercalations of the Karahidir volcanics in the violet conglomerate (Fm2) are observed. The volcanics are most abundant in the southern part of the basin, where they are thrust over the sedimentary sequence.

The volcanics are reworked in the several conglomerate occurrences in the sedimentary sequences of the basin. The volcanics are assumed to be of Pre-Maastrichtian – Paleocene age (Göncüoğlu *et al.*, 1993). Radiometrically dating yielded a ^{40}K - ^{40}Ar age of 71.68 ± 2.24 Ma (Van Hinsbergen, personal communication, 2011).

Lower Group



Figure 7. Lenticular sand body in black sheared clays (Fm1). Hammer for scale.

Fm1. Black clays

The base of the sedimentary succession is formed by a alternating sequence of dark-coloured clays and sandstone with a minimum thickness of 250m. This unit only crops out in the central part of the basin, where the exposed thickness is a 250m, and tapers out to the west, where the thickness is only 1-3 m. In both cases the sequence is adjacent to the volcanics and is sheared (see figure 7).

In common the beds are thin bedded, ranging in thickness between 10 - 20 cm.

The sequence is interpreted as a fluvial environment.



Figure 8 Flute casts. Photograph shows bottom of an overturned bed of violet conglomerate. Flute casts at the lay side of the pebbles indicate a flow to the top left of the photograph. Tilting to original orientation indicates paleoflow to the south.

Fm2. Violet Conglomerate

Violet and red conglomerates and intercalated sandstones form a sequence, exposed in the southern and south-western part of the basin, with a thickness of around 600 m in the south-eastern part, and up to 825 m in the south-western part. At the west bank of the Kızılöz river, intercalations of the Karahidir volcanics in the base of the violet conglomerate (Fm2) are observed. The formation tends to become finer grained upward and is essentially made of two types of lithologies:

- Clast-supported conglomeratic layers, with sub-angular volcanic clasts varying in size between 10-50 cm. The bed thickness of these conglomeratic layers varies between 1 and 5 m. The conglomeratic layers often show erosional contacts into underlying sandy layers, with lenticular bodies, that cut down to 1 m into the underlying sediments. Clasts near the base of the formation consist mainly of mafic to intermediate volcanics (95%) and some dark green to bluish volcanic glass.
- Matrix-supported sandy layers, with volcanic granules. The bed thickness of the sandy layers never exceeds about 1 m, and most of the layers are about 20-30 cm thick.

Within these sandy layers, there is sometimes a thin bed (10-20 cm max.) of fine-grained conglomerate with pebbles less than 5 cm diameter. Towards the top of the formation, the contrast between the sandy and conglomeratic layers decreases, because the pebbles in the conglomerate are smaller. A majority of the pebbles range in size between 2-5 cm, and only few are larger than 10 cm. In addition, upward in the sequence a higher proportion (about 25%) of the pebbles is composed of glassy volcanics. Paleocurrent directions in this formation are variable. Crossbedded structures in the southeastern part of the basin indicate westward flow, whilst flute casts in the central part of the basin indicate south-directed flow (see figure 8). The unit is interpreted as alternating braided fluvial and debris flow deposits constituting a continental clastic fan system.

Fm3. Sandstone and blue clays

The violet conglomerate is unconformably overlain by an up to 1185 m thick sequence of sandstones and blue clays, lying at an angle of about 15° to the underlying conglomerate. The sequence tapers out to the east, where it is exposed in small lenses only.

The sequence comprises a yellow-coloured sandstone member (*Fm3-a*) at the base with a thickness of about 150 m, consisting of a regular alternation of approximately 30 cm thick yellow-weathered and carbonate-rich, fine- to medium-grained sandstone intercalated with 2-4 m thick silts and clays. The yellow sandstone member is followed by a more than 1000 m thick sequence made up of regularly alternating thin-bedded blue claystone and equally thin-bedded very fine-grained yellow sandstone (*Fm3-b*). The beds are between a few centimeters and 15 centimeters thick.

Both in the sandstone member and in the overlying blue clays, slump structures are visible (figure 4.a). In the sandstone member there are rotated syn-sedimentary normal faults indicating a roughly E-W direction of extension (figure 4.b)

The sandstone is interpreted as a fluvial environment and the blue clays are interpreted as a lacustrine environment.



Figure 9. Both pictures looking east, younging direction N (left side of figures). (a) Left, syn-sedimentary slumping. Deformed layers within a formation covered by undeformed layers. (Douwe for scale). (b) Right, syn-sedimentary faulting. Thickness of same beds differ, covered by non-faulted beds.

Fm4. Pale Red Sandstone and Conglomerate

The sandstones and blue clays are overlain by a sequence with a fairly constant thickness of about 625 m of red sandstones. In the western part of the basin, the base of the succession consists of medium- to coarse-grained, thick-bedded (1-2 m) grey sandstone layers. Higher in the stratigraphy, fine- to medium-grained laminated sandstones occur in beds of 5-15 cm thick, intercalated with 5-50 cm thick beds of red silt. In the eastern part of the basin the unit consists of irregularly alternating conglomerate, coarse sand and silt. Pebbles in the conglomerate mainly consist of andesite.

The sequence is interpreted as a fluvial environment with braided rivers represented by the conglomeratic layers and channel fills represented by the silt layers.

Middle Group

Fm5. Dark Red Sandstone

The Pale Red Sandstone and Conglomerate are unconformably overlain by a sequence of dark red sandstone with a thickness of about 400 m. This sequence becomes thinner towards the eastern part of the basin, where it is about 200 m thick.

The sequence comprises a white coloured sandstone member (*Fm5-a*) of 20 m thick, consisting of very coarse sands. The white sandstone member is followed by a poorly exposed sequence of fine laminated dark red sands (*Fm5-b*). The top of the formation is formed by intercalations of fine bedded silty sand and clay (*Fm5-c*).

The sequence is interpreted as a transition from a fluvial environment represented by the sandstones to a lacustrine environment represented by the silty sand and clay.

Fm6. Limestone

The dark red sandstone is in the eastern part of the basin overlain by a 100 m thick sequence of limestones. The limestone consists of 1-2 m thick beds of very fine grained calcareous mudstones, without macroscopically observable fossils.

The sequence is interpreted as a lacustrine deposit.

Fm7. Orange sandstone

The lacustrine limestones are overlain by a 250 m sequence of sandstones and shales. The relation with respect to the underlying limestones is unknown, since the only contact with the limestones is a thrust fault contact.

The sequence consists of a regular alternation of 5-15 cm thick carbonate-rich sandstone layers and 15-30 cm thick shale layers with an exposed thickness of 20 m (*Fm7-a*). This alternation of sands and shales is followed by a 230 m thick sequence characterized by 0.5-2 m thick beds of coarse sands (*Fm7-b*). These beds show large-scale crossbeds (see figure 10). The sequence is interpreted as a fluvial environment.

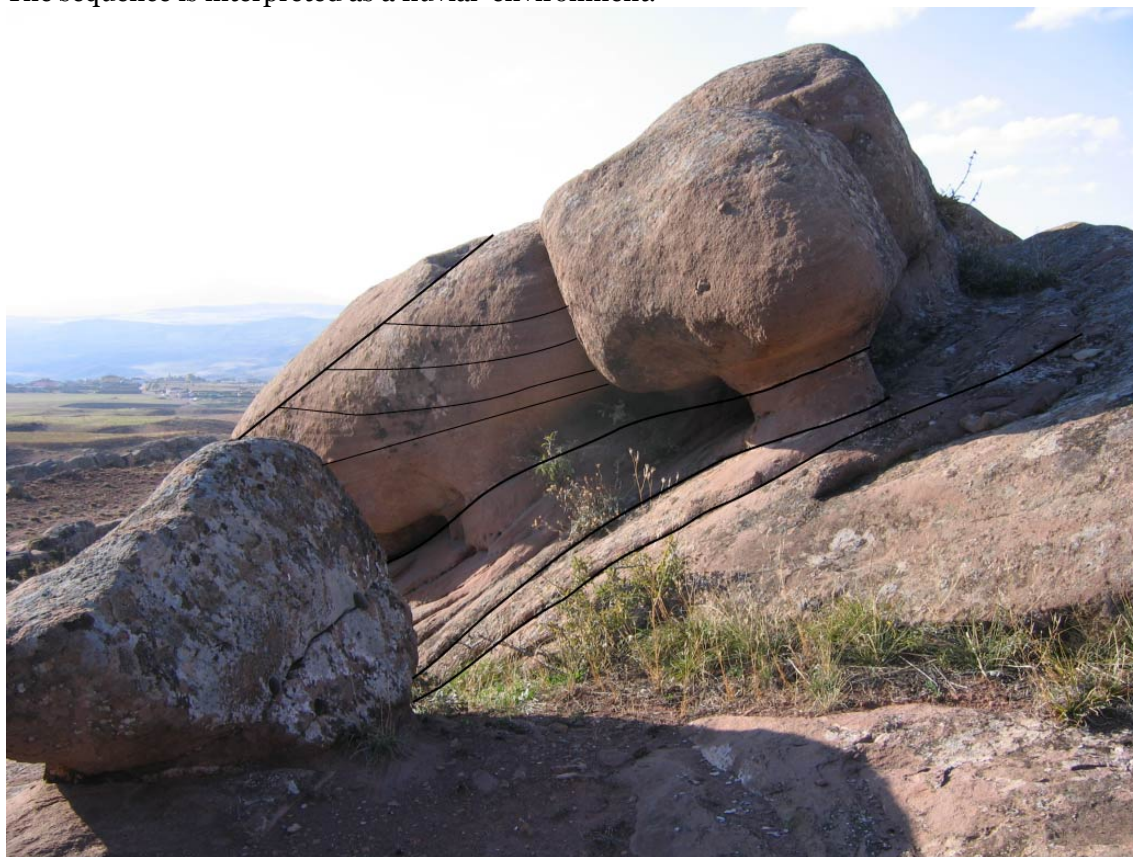


Figure 10. Large scale crossbeds, vertical thickness about 2m.

Fm8. Nummulitic limestone

The sandstones are unconformably overlain by a 200 m thick sequence of limestones, lying with an angle of about 5° with respect to the underlying sandstone (see figure 11). The sequence consists of a variable alternation of 0.5-1 m thick, grain-supported beds of nummulites and thick (about 10 m) beds of oysters and nummulites.

The fossil content demonstrates a shallow marine deposit.



Figure 11. Angular unconformity between nummulitic limestone (above thick line) and underlying sandstone. View of photograph to SW.

Fm9. White marls/clays

The nummulitic limestone is overlain by a ~ 100 m thick sequence of white marls and clays. The relationship with the underlying limestone is not known, since the only exposed contact is a thrust fault contact.

The sequence consists of a variable alternation of 2 m thick carbonate-rich sandstone beds and 5-20 cm thick layers of claystone and carbonate. The outcrops of this sequence show spectacular examples of syn-sedimentary deformation such as slumping (see figure 19b).

The sequence is interpreted as a lacustrine environment.

Upper Group*Fm10. Conglomerate & Lignite bearing shales*

The lower and middle units are unconformably overlain by a monoclinial succession of at least 450 m thick sequence of dark red conglomerate and shales, having a northward dip of 50° at the very base of the sequence to an average of around 30° higher in the sequence. The sequence comprises a 150 m thick conglomerate member (*Fm10-a*) at the base. The succession consists of two type of layers:

- Conglomerate layers almost entirely consisting of boulders ranging in size between 5-30 cm, with only 10% (or less) matrix. The clasts comprise metamorphic rocks and granites.
- Sand layers consisting of fine- to medium-grained sandstone. In these layers small scale slump structures are visible.

Both imbrication of the pebbles in the conglomeratic layers and crossbeds in the sandy layers indicate eastward directed paleoflow (see figure12).



Figure 12. Imbricated pebbles in Fm10, indicating an eastwards paleoflow. View of photo to N.

The conglomerate member is followed by a 300 m thick sequence of 5-20 cm thick fine grained sandstone beds intercalated with 5-50 cm thick lignite bearing shale beds (*Fm10-b*). The sequence is interpreted as an alternation of braided fluvial and debris flow deposits constituting a continental clastic fan system. Upward in the sequence the environment changes to become dominated by fluvial deposits and marshes.

Fm11. Fluvial sands

The lignite bearing shales are overlain by a 300 m thick sequence of sandstone and clay. The sequence comprises a 100 m thick sandstone member (*Fm11-a*) at the base. This member consists of very coarse to granular olive-greenish sandstone beds of 1-2 m thick, with crossbeds. The sandstone member is followed by a 200 m thick sequence of a regular alternation of 20 cm thick fine-grained sandstone beds and 0.5-2 m thick clay layers (*Fm11-b*). Lens-shaped sand bodies, 5-10 meters thick and 20-30 m wide, float in this sequence. Crossbeds in the sandstone layers indicate paleoflows to the west.

The sequence is interpreted to reflect a fluvial depositional environment, with channelled sandstone bodies and clay as overbank deposits.

Fm12. Orange conglomerate

The fluvial sandstone and clays are overlain by a sequence of orange weathered conglomerate. This conglomerate consists of two type of layers:

- Matrix supported conglomerate layers of up to 3 m thick. These layers have moderately sorted, semi-rounded pebbles ranging in size between 4 to 10 cm. The pebble content is diverse, in the lower part of the sequence mainly volcanics and some reworked sandstone, but higher in the sequence (near Sarılar) also fragments of nummulitic limestone occur.
- Sandstone layers of 20 cm thick, with grainsizes between medium and very coarse sand.

At the base of the succession, pebble imbrication and crossbeds indicate east directed paleoflow.

The unit is interpreted as an alternating braided fluvial and debris flow deposit making up a continental, alluvial fan system.

AGE OF SEDIMENTS

The age control of the sedimentary rocks is poor. Continental sediments are hard to date and in this basin, none of the continental deposits are dated. Unfortunately, dating of the lignites in the Upper Group and clays throughout the whole sequence of the basin gave no results. Without these dates, the age of the sediments can only be constrained poorly. The volcanics which overlie the metamorphic basement are of Campanian-Maastrichtian age (71.68 ± 2.24 Ma) (*Van Hinsbergen, personal communication*). The Nummulitic limestone (Fm8) is of Middle Eocene (Lutetian: 48.6 ± 0.2 to 40.4 ± 0.2 Ma, *Gradstein et al. 2004*) age, which is based on the fossils *Alveolina* sp. and *Nummulites* sp. (*Göncüoğlu et al. 1993*). This constrains the deposition of the complete Lower Group and part of the Middle Group to at largest 33.7 million years and at shortest 20.6 million years. The orange conglomerate (Fm12) of the Upper Group is covered by volcanics rocks commonly referred to as the Ürgüp formation, which is dated at 11.2 ± 2.5 to 9.0 ± 0.4 Ma (*Mues-Schumacher and Schumacher, 1996; Viereck-Goette et al., 2010*). The deposition of the latest part of the Middle Group and the entire Upper Group can be constrained to a time span of 26.5 to 40.2 million years.

4. STRUCTURE

NORTHERN PART

The northern part (see figure 13, sub-area 1.) of the Ayhan region is characterised by a north dipping succession with an erosive base. The dip of the stratigraphy varies from occasional dips of up to 50° N at the base of the succession to values ranging between 25° and 35° N further north.

Figure 13. (page 17.) Map with sub-areas. Per sub-area equal area stereoplots are shown, indicating number of measurements, average dip and average fold axis.

Figure 14. Balanced cross-section and restoration through the Ayhan Basin. For location of cross-sections and key, see Geological map (Appendix 1). All cross-sections are constructed using line length balancing. The section are restored to the horizontal base of Fm5. Since no normal contacts between Fm 5/6 and Fm 7 are exposed, we assumed a normal contact relationship, without angular unconformities. The small angular unconformity between Fm 7 & 8 is not shown in the sections.

- (a) **Cross-section A. Original cross-section: angular relations between layers are consequently extrapolated to depth. Restoration: Metamorphic rocks of Hırkadağ are not shown, since they are at depth at the moment to which is restored. No significant net shortening, but only tilting is observed between original and restored section.**
- (b) **Cross-section B. Original cross-section: angular relationships between formations of cross section A are assumed. Note that most shortening is accommodated in the footwall syncline at the south. Restoration: position of Fm2 below the central part of the section serves to illustrate general structure.**
- (c) **Cross-section C. Note that the fold- and thrust zone accommodates the most shortening, and the monocline structure (dominated by Fm2) at the south shows net extension.**

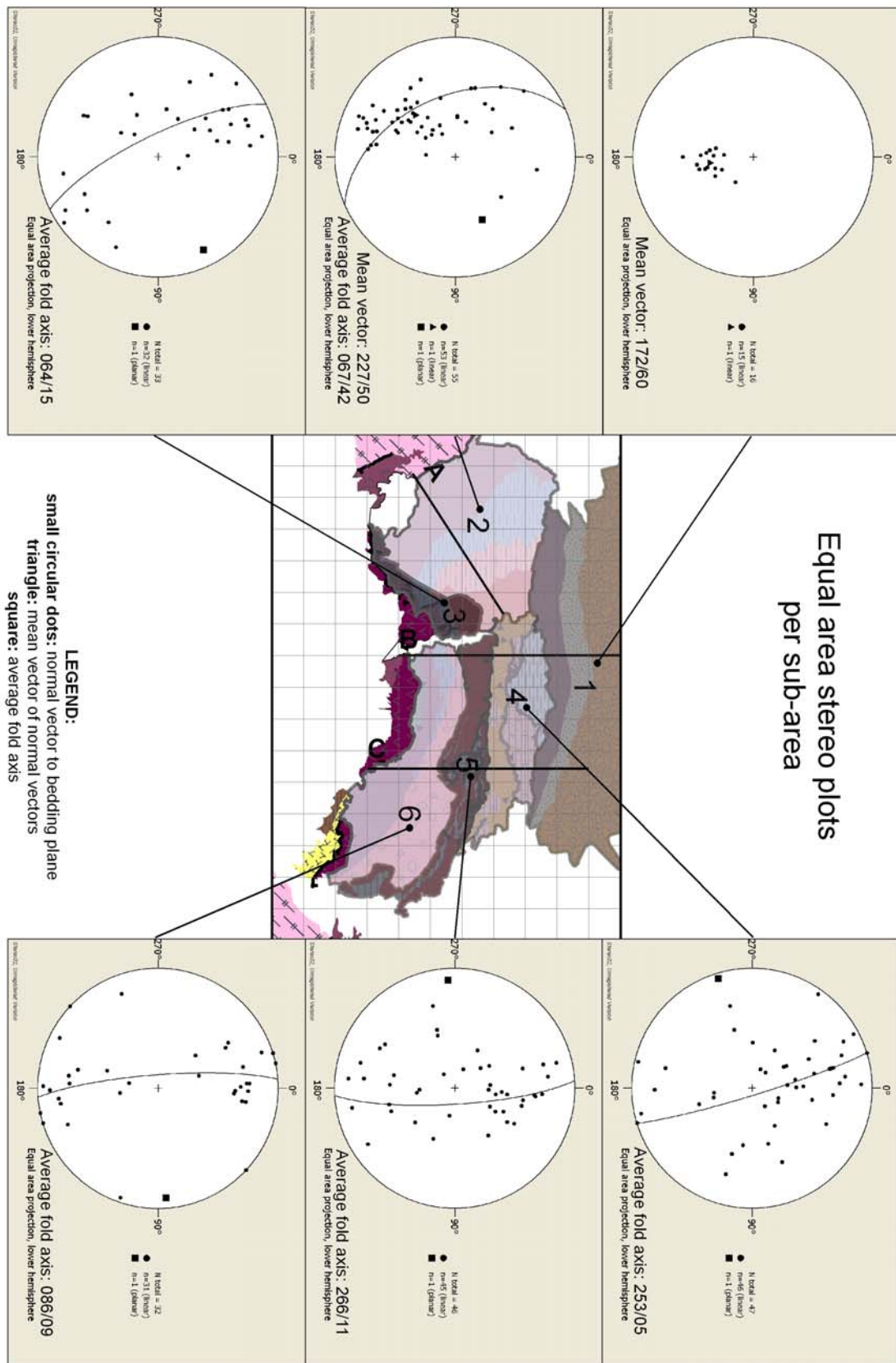


Figure 13.

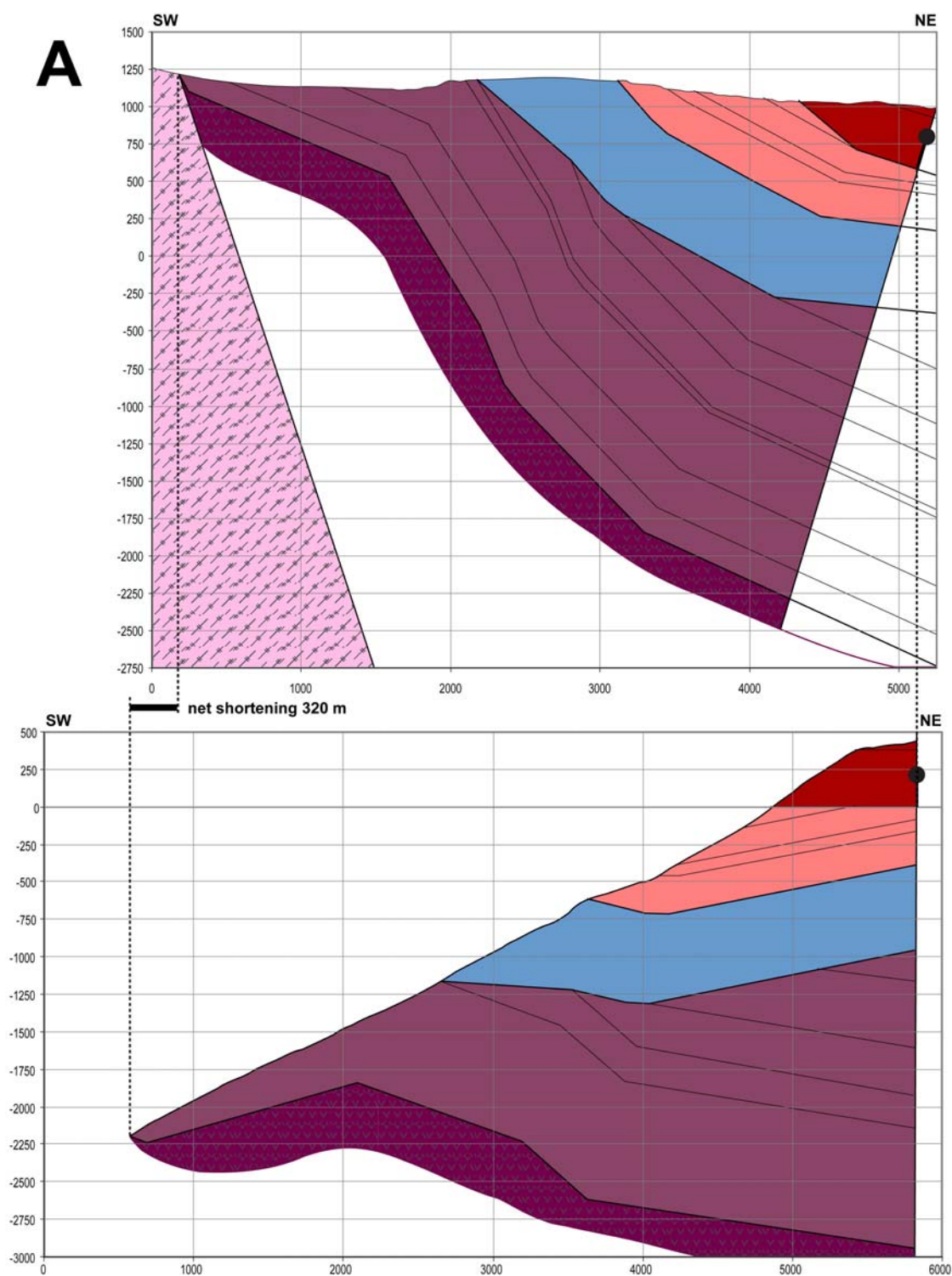
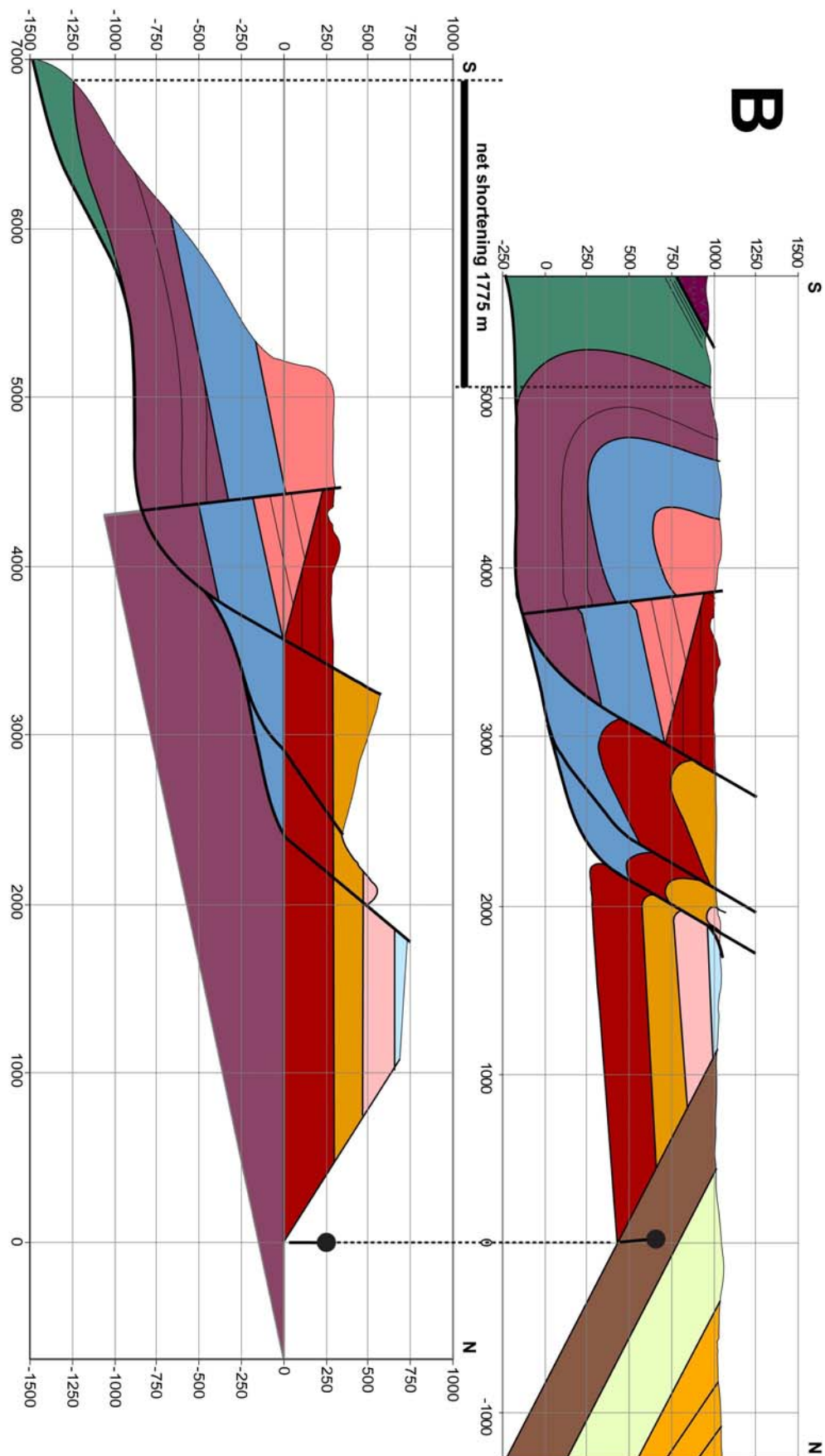
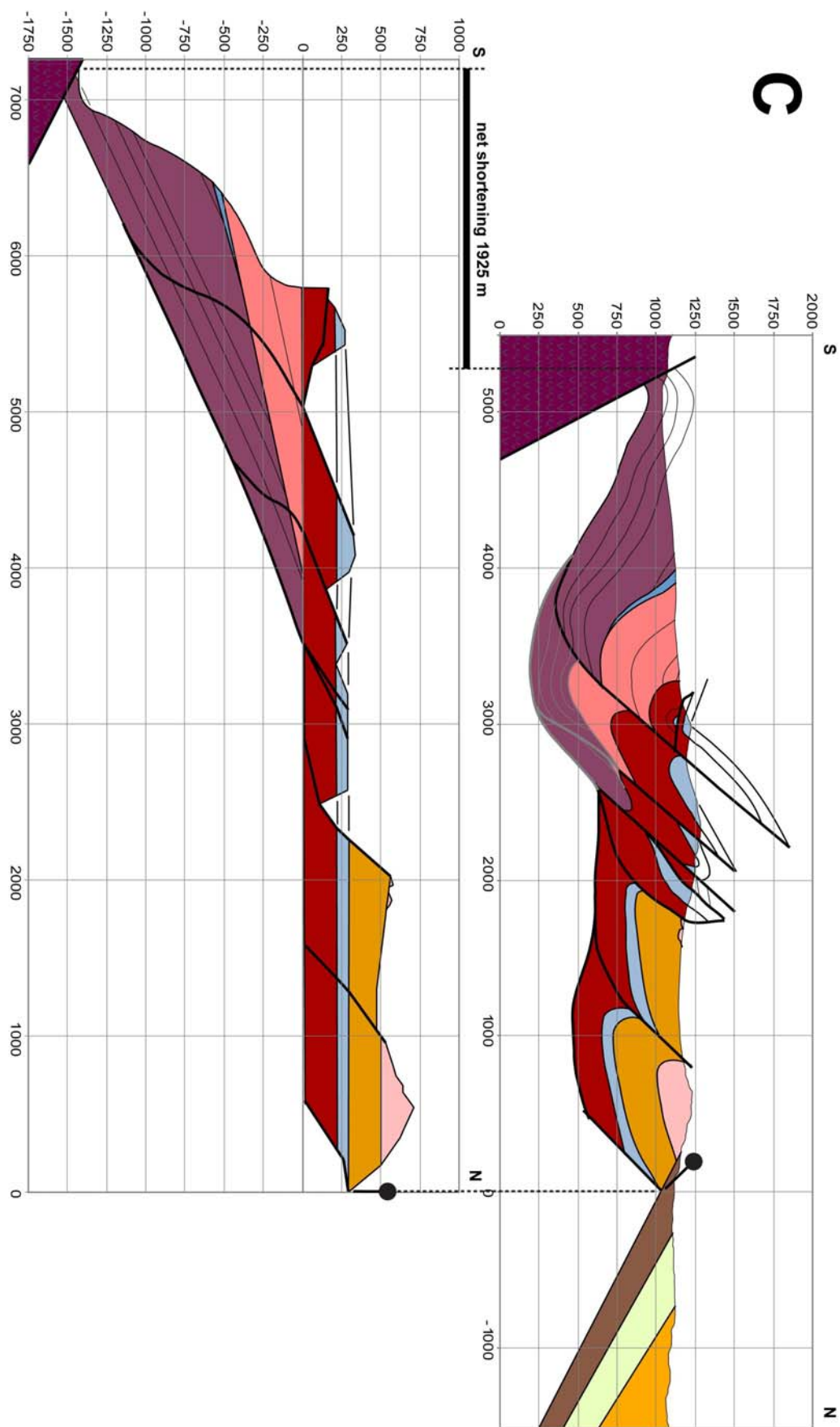


Figure 14.





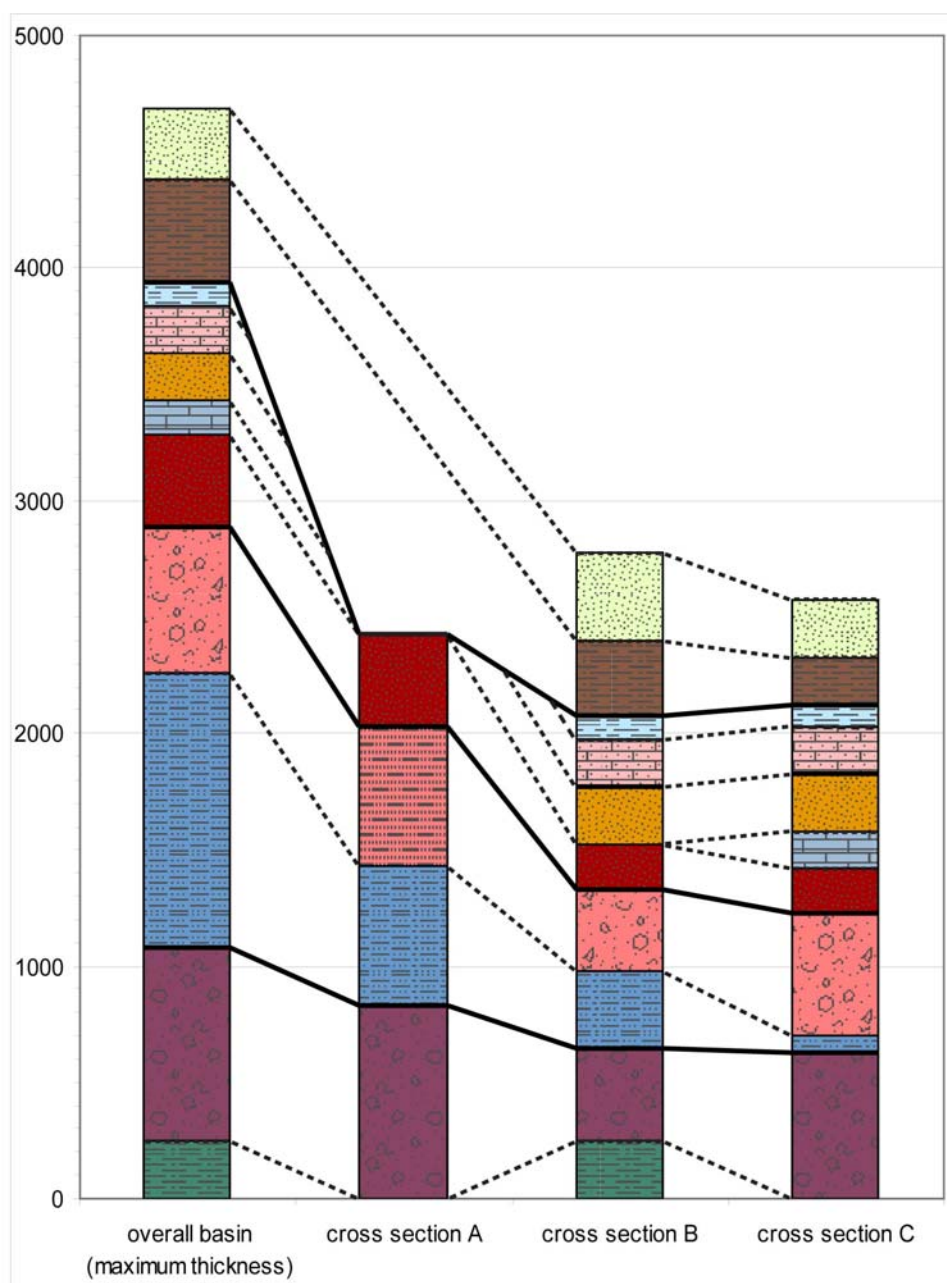


Figure 15. Stratigraphic correlation chart. Stratigraphic thickness along profile lines A, B, C on Geological map (Appendix 1.). Heavy lines are unconformities, dashed lines denote correlations of the formations through the different sections.

WESTERN PART

The western part (sub-area 2, see figure 13) is located next to the metamorphic Hirkadağ block, from which it is separated by a steep ENE dipping normal fault. The adjacent layers of violet conglomerate (Fm2) show an increase in dip from 25° to 70° towards the fault, in line with drag folding.

The western part is a NE dipping monoclinical succession. Due to angular unconformities the dip of the layers varies significantly.

In the northwestern part of this domain, small scale (1-10m) WSW-ENE oriented tight folded synclines and anticlines occur (see figure 16), indicating roughly N-S directed shortening. On

large scale, the outcrop patterns of Fm 2 & 3 also show a km scale syncline and anticline with steeply dipping fold axes (see Appendix 1).



Figure 16. Tight folded sandstone layers in Fm3 in the northwest corner of sub-area 2. Hammer for scale. View of photographs to W.

Cross section A (see figures 14a) serves to illustrate the monoclinial structure. No significant net shortening can be observed, only tilting. The restored section shows open folding of the violet conglomerate. Because of the minor deformation in the section, stratigraphic relations (e.g. angular unconformities) between the different units are clear, and these relationships are assumed to be equally valid in the more deformed parts of the basin.

In the southwest (sub-area 3, see figure 13), inverted normal faults are present (see figure 17.), indicating extension during or after deposition of the blue clays and the pale red sandstone. This inversion is probably related to thrusting of the volcanics in the south. In Fm3, syn-sedimentary normal growth faults are present (see figure 9b), indicating a roughly E-W extension.

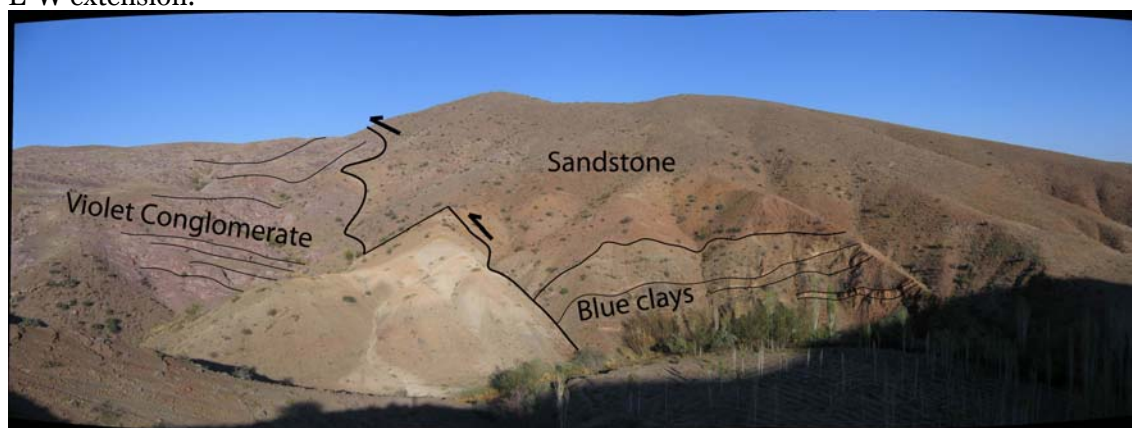


Figure 17. Inverted normal fault. Left of fault Violet Conglomerate (Fm2), right of fault Blue clays (Fm3-b) and sandstone (Fm4), thrusting over older units. Width of view about 250 m. Center of view towards 070 (ENE).

Towards the south the dip of the sediments increases to almost vertical and they are in places overturned. The orientation of the layers gradually changes from NE dipping (strike 140°) to N or S (strike 100°).

To the south, the basin is almost entirely bounded by volcanic rocks. In the west these volcanics, together with slivers of granite and metamorphic basement, are thrust over the sediments (see figure 18). The edge of the thrust sheet between village of Yesilöz and the Kızılöz river shows transfers in the outcrop pattern (see geological map, Appendix 1). Duplexes with an oblique sense of motion and sinistral strike slip faults in the sediments coincide with these transfers. Along the contact of the thrust sheet, the sediments are more intensively deformed towards the east.

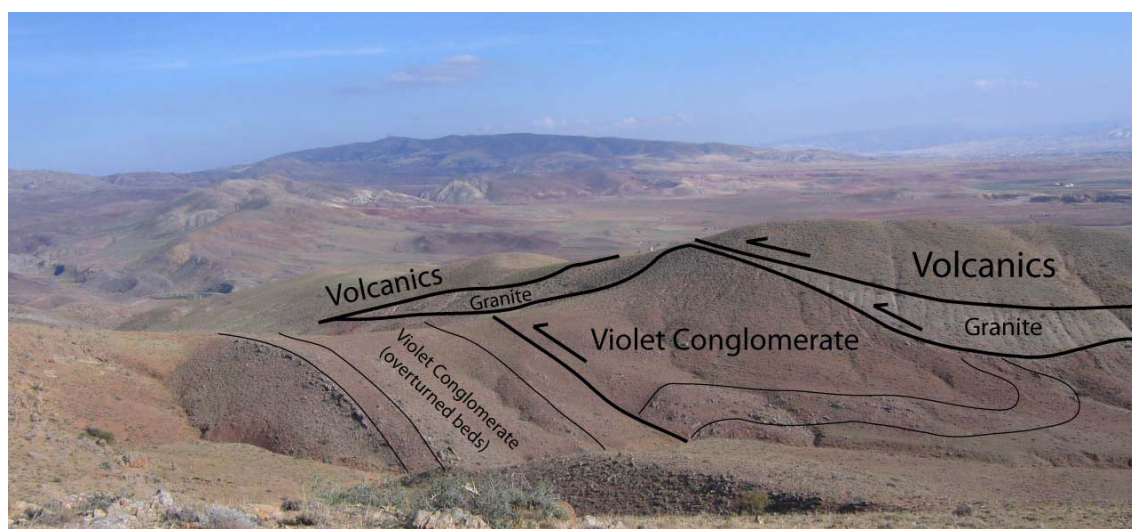


Figure 18. Volcanics and granite slivers thrusting over sediments (Fm2). Note the duplex structure in the sediments.

CENTRAL PART

The structure of the central part (western parts of sub-areas 4,5 and 6, see figure 13) are shown in cross-section B (figure 14b). Below the thrust sheet of volcanics, a footwall syncline structure with an overturned southern limb is present. Further north (sub-area 5 & 6), however, a normal fault again points to an earlier stage of extension.

The northern border of the exposed dark red sandstone (Fm5) is formed by a thrust fault. Thrust faults form a piggy back structure in sub-area 4, comprising two fault bounded blocks. Near the Kızılöz river, only footwall synclines are observed.

The total shortening in cross section B is 1775 m.

North of this piggy back structure, part of the frontal ramp is composed of marl (Fm9). These marls show a variety of deformational structures: E-W trending, 10-50m scale chevron folds (see figure 19a), with steeply dipping northern limbs and shallowly dipping southern limbs, and an axial plane dipping $\sim 45^\circ$ S. The enveloping surface of these folds is roughly horizontal. Syn-sedimentary deformation indicating slumping is also present (see figure 19b): Within the sequences, isoclinal folding occurs which is cut of by the same lithology.

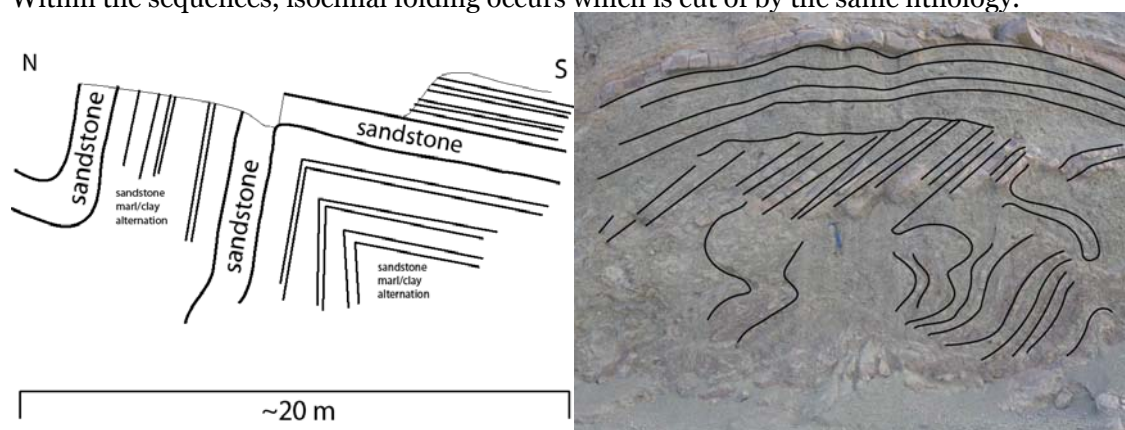


Figure 19. (a)Left: Chevron faults in the white marls/clays

(b)Right: Syn-sedimentary deformation in white clays/marls. Deformed, isoclinally folded layers are covered with less deformed layers of the same unit. Hammer for scale.

EASTERN PART

The structure of the eastern part of the basin is illustrated in cross section C (see figure 14c). Volcanics (unit V III) occur to the south and are bounded by a $\sim 55^\circ$ N dipping normal fault (see figure 20). The violet conglomerate (Fm2) is gently folded, similar to the folding in the western part of the basin. North of the violet conglomerate, a lense of blue clays (Fm3b.) unconformably overlies the violet conglomerate. The sequence ends with almost isoclinally folded dark red sandstone (Fm5) and lacustrine limestone (Fm6) with vertical limbs. This isoclinal syncline is covered by a back-thrusted pop up structure comprising the same stratigraphic units.

North of this pop-up structure, a fold-and-thrust structure occurs, showing both footwall synclines and hanging wall anticlines in the dark red sandstone and the lacustrine limestone. North of this structure, a piggy back structure similar to the structure in the central part occurs, comprising two fault bounded blocks in the sands (Fm7) and nummulitic limestone (Fm8). Again, only footwall synclines are exposed here. The synclines have a shallow west plunging fold axis.

The total shortening in cross section C is 1925 m.



Figure 20. Normal fault contact between volcanics (KV) (right) and Violet Conglomerate (Fm2) (left). View of photograph to the east.

5. DISCUSSION

GEOLOGICAL HISTORY

The volcanic rocks, identified by *Göncüoğlu et al. (1993)* as the Karahadır volcanics, form the floor of the basin. This is observed in the western part of the basin, where these volcanics underlie the violet conglomerate (see also cross section A). At the west bank of the Kızılöz River, the violet conglomerate (Fm2) overlies the volcanics and some intercalations of the

volcanics in the violet conglomerate occur at the base of Fm2. This indicates that volcanisms was still active during deposition of the first two formations (Fm 1 & 2). At the east bank of the Kızılöz River, the base of the sedimentary sequence is formed by black clays with intercalated sand bodies (Fm1). This formation is also exposed at the western boundary of the basin, overlying the volcanics. During the active volcanism the basin formed and subsided, creating accommodation space for a fluvial or lacustrine deposit.

The violet conglomerate represents a thick continental alluvial fan deposit, presumably deposited directly after initial basin formation by tensional faulting, as suggested by *Göncüoğlu et al. (1993)*. These authors identified the Karahıdır volcanics as the Göynük Volcaniclastic Olistotrome in the İdis Dağı area some 10 km east of the study area. In the Hirkadağ area, no such olistotrome occurs, and the volcanics are only found as boulders of <50cm in the violet conglomerate. Higher in the sequence sand layers become more abundant and the clasts in the conglomerate (Fm1) are reduced in size, suggesting a decrease in relief.

Since the violet conglomerate (Fm2) is gently folded, as shown in cross section A and forms a taper to the normal fault, as shown in the restoration of cross section B & C, a first stage of extension must have taken place during its deposition.

The folds could represent fault ramp synclines or fault bend anticlines, caused by a ramp-flat fault geometry (*Twiss & Moores, 1992*). This deformation is also indicated by the angular unconformity between the violet conglomerate and the overlying sandstone member. Although the orientation of the unconformity varies, we note that the angle of the unconformity is about the same throughout the research area.

After this first stage of deformation, the basin experienced subsidence and the violet conglomerate is unconformably overlain by sandstones and blue clays (Fm3).

When retitled to the original orientation, the syn-sedimentary normal faults in the steeply N-dipping Fm3 in sub-area 3 suggest a component of E-W extension during the deposition of these sediments.

Pale red sandstone and conglomerate (Fm4) cover the blue clays (Fm3). The further development of the basin, however, was marked by continuous tectonic activity, as suggested by the repeated development of unconformities. The pale red sandstone and conglomerate (Fm4) are unconformably overlain by dark red sandstone (Fm5). The very fine to silty grain size of the sands and the lacustrine limestone (Fm6) on top of the sandstone points to a very quiet depositional environment. This was followed by a phase of normal faulting possibly accommodating ongoing subsidence of the basin as indicated by the overlying sands (Fm7). Subsidence brought the basin eventually below sea level, hence the deposition of marine nummulitic limestones (Fm8).

The development of thrust faults affecting much of the area clearly indicates a change in tectonic regime, and many of the above units are affected by N-S directed shortening.

The conglomerates (Fm10) at the base of the Upper Group of units, which unconformably cover the basin in the north, contain large boulders of metamorphic and igneous rocks, indicating a very proximal source. These conglomerates represent the earliest stratigraphic level characterized by widespread coarse metamorphic detritus. The conglomerate is overlain by sediments suggesting a quieter depositional environment, but the highest unit of the Upper Group is again made up of (orange-coloured) conglomerate (Fm12). At the base it only contains metamorphic and igneous detritus, but higher in the sequence there are also clasts of nummulitic limestone (Fm8).

PALEOGEOGRAPHIC STRUCTURE

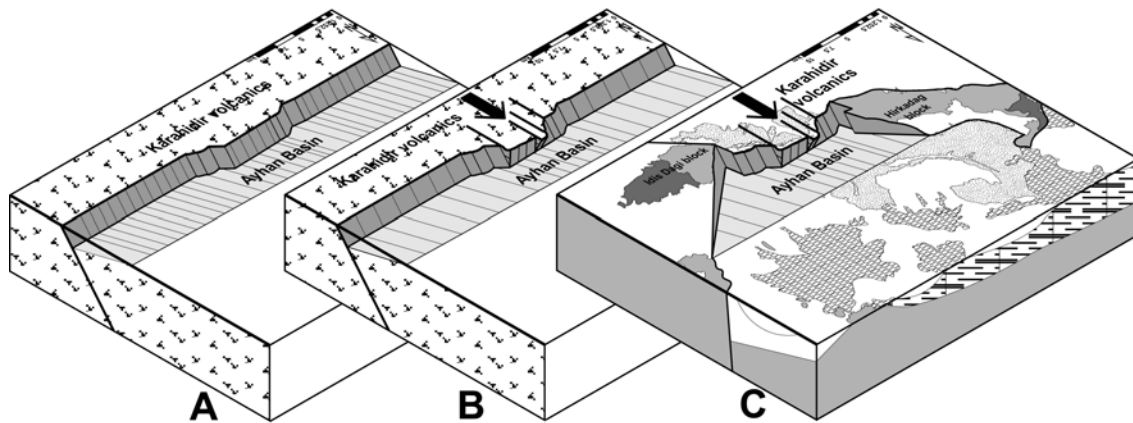


Figure 21. Schematic block diagrams showing the paleogeographic extent of the basin. (A) Situation direction after tensional faulting, (B) situation during thrusting (post-Lutetian), (C) present-day situation. Key as in figure 4.

The restoration of the all the cross sections show that the thickness of the sedimentary sequence (especially the Lower Group) increase in thickness towards the south. This could indicate that the basin is formed as a half graben with an N-S oriented extension, which is bounded at the south by a N-dipping normal fault (see figure 21).

The lateral variation in stratigraphic thickness of the Lower Group indicates that the depocenter of the basin was located in the SW. The drag-folding of the lower units (Fm 1 & 2) along the Hırkadağ fault, indicate that these covered this block, before activation of the fault. So the basin was in the initial configuration much larger towards the W and E than what is now preserved. This is supported by Köksal & Göncüoğlu (1997), who found a sedimentary basin covering the N-side of the İdis Dağı block with a similar stratigraphy (see figure 3b) and geological evolution.

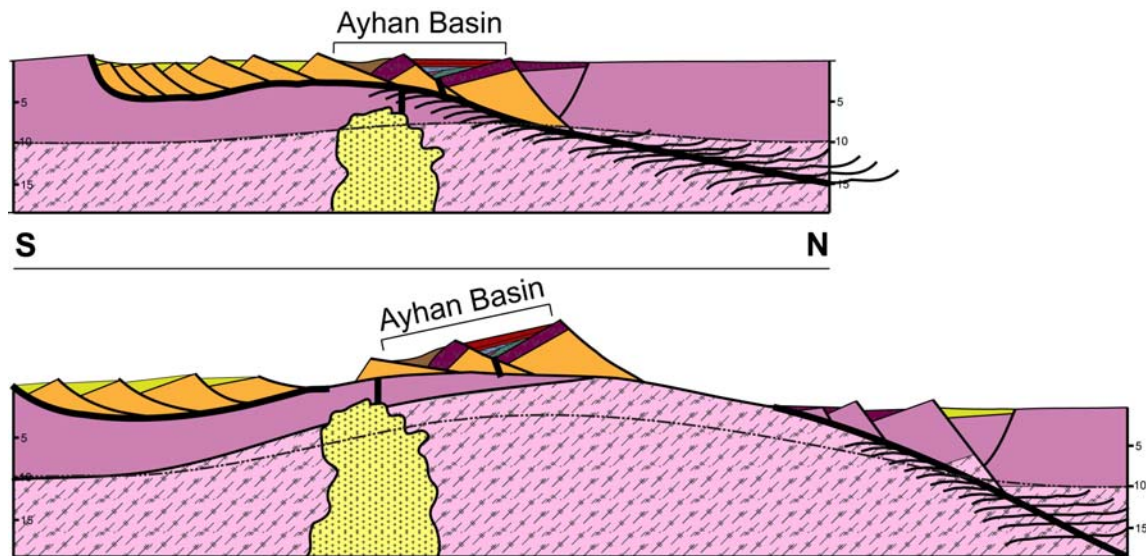


Figure 22. Klippe structure on a metamorphic core complex. During extension, a low angle detachment fault cuts through the upper and lower crust. A klippe structure may form when part of the hanging wall is transported as a passive rock body on top of the footwall.

On top of the Hırkadağ block, a low angle detachment fault with a top NE movement sense is observed (Lefebvre, personal communication, 2011), which juxtaposes sheared mylonitic

metamorphic basement to brecciated violet conglomerate (Fm2). This indicates that the Ayhan Basin is a supra-detachment basin.

The basin is proposed to be a 'extensional klippe'. Such an extensional klippe is formed when a part of the hanging wall breaks off and is transported on the footwall as passive rock body during activity of the extensional detachment (*Van Hinsbergen & Meulenkamp, 2006*) (see figure 22). The arguments to determine the Ayhan basin as an extensional klippe are:

- 1.) The isolated occurrence of this basin. No similar basins are found in the near region (except for the basin north of the İdis Dağı block).
- 2.) The basin is entirely fault bounded and surrounded by footwall material and younger deposits that postdate the extension.

TIMING OF TECTONIC EVENTS

Most tectonic events are not only visible as tectonic features such as folds and faults, but are also represented by other geological features, such as angular unconformities and detritus in sedimentary layers. (e.g. the initial faulting of the Karahıdır volcanics is represented by the volcanic detritus in the violet conglomerate.)

Faulting

The timing of most minor extensional faults is determined with certainty. Both the structure (syn-sedimentary faults and syn-sedimentary deformations structures) and the interpreted facies of the units both indicate subsidence and extension. The same holds for the compressional faults.

It is difficult to date the activity of the faults at the west and east that now form the boundaries of the Ayhan Basin. It is assumed that these faults became active in the latest history of the basin, based on the following arguments:

- 1.) The orientation of the faults seems not affected by tilting. Both faults are steeply dipping ($\sim 70^\circ$).
- 2.) The drag-folding of the overlying sediments (Fm 1 & 2) indicate that the Hırkadağ block was covered by these sediments, before faulting occurred.
- 3.) The Hırkadağ fault does not show signs of large displacement.

Tilting

The Upper Group unconformably covers the rest of the basin at the N, with a large angle w.r.t. to the underlying strata and w.r.t. the present day horizon. This clearly indicates that tilting has occurred before deposition of the Upper Group. Based on the geometry of the thrust faults, the tilting must have postdated the thrusting, otherwise the faults become inversed. Since the Upper Group is now tilted north, the basin must have tilted back to its present day position during or after deposition of the Upper Group. The mechanisms by which this could be accommodated are not known and are subject for future research.

A possible scenario could be a large scale listric fault south of the basin (see figure 23.). N-S extension caused S-wards tilting of the basin. An inversion of this fault creates N-wards retilting. There is no proof for this scenario and if such a fault exists, it is probably buried under the Cappadocian volcanic deposits, which make it hard to collect evidence for this scenario.

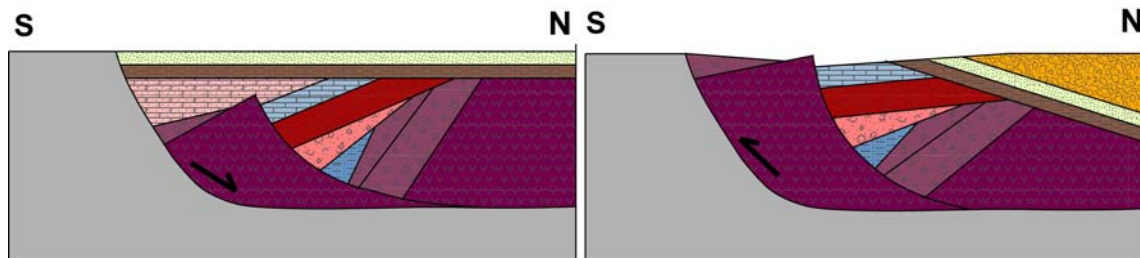


Figure 23. Schematic diagram showing an hypothetical explanation for the double tilting of the Upper Group, as result of listric faulting (left) and later reactivation of this fault (right).

Exhumation

On regional scale, the CACC is unconformably covered by Eocene sediments, indicating that the rocks were already exhumed and unroofed ('exhumation' in this case is the motion of the rock towards the surface, and 'unroofing' restricts to the stage where the rock is at the surface and being eroded; terminology after *Gautier et al. (2002)*) before deposition of these sediments. This is supported by radiometric cooling ages of the igneous and metamorphic rocks in the study area (*Lefebvre, personal communication, 2011*), which are in line with the results of *Boztug et al. (2009a)* and *Boztug & Jonckheere (2007)*.

The mechanism of exhumation of the metamorphic rocks is also established in the study area: brecciated conglomeratic rocks of Fm2 are found in a low angle detachment fault contact overlying sheared and brecciated metamorphic rocks (*Lefebvre, personal communication*). This contact has a top towards NE movement sense.

However, in the study area there is no proof for pre-Eocene unroofing. The stratigraphically lowest occurrence of macroscopically sized metamorphic detritus is found in Fm10, which forms the base of the Upper Group. Thus, we can only date the unroofing in the study area to be post-Lutetian. future research should focus on the microscopic petrography of the sediments, to determine the age of unroofing more exactly.

6. CONCLUSIONS

- The Ayhan basin is formed as an extensional basin, as evidenced by the steep dipping normal fault which forms the southern boundary of the basin. The formation of the basin occurred during the emplacement of the Karahidir volcanics (71.68 ± 2.24 Ma).
- The Karahidir volcanics form the floor of the basin, evidenced by the nonconformably overlying black clays and violet conglomerates and intercalation of volcanics in this violet conglomerate.
- The basin is characterized by pre-Lutetian syn-sedimentary extension, evidenced by syn-sedimentary normal faults.
- N-S directed compression started after the Lutetian. During this compression, the basin is deformed by folds and south-dipping thrust-faults. The volcanics at the southern boundary of the basin are thrust northwards over the sedimentary sequence.
- After this compression the basin is southwards tilted and uplifted. North-dipping clastic sediments are deposited, which unconformably overly the Campanian-Lutetian sediments of the Ayhan basin. After deposition the post-Lutetian sediments retitled N-wards. The mechanism by which this is accommodated is not known.
- Exhumation of metamorphic rocks in the study area is accommodated by a low angle detachment fault with a top NE movement sense.
- Unroofing of metamorphic rocks in the study area is only recorded in the Upper Group, at the base (Fm10-a). Thus, in the study area, the unroofing can only be dated to be post-Lutetian. This is opposed to the regional geology of the CACC, where unroofing occurred during the Eocene, as evidenced by unconformably overlying middle-Eocene sediments.

7. ACKNOWLEDGEMENTS

This work is supported by a grant from Stichting Molengraaf Fonds. I would like to thank Reinoud Vissers, Douwe van Hinsbergen and Côme Lefebvre for their help in the field and reviewing the results and manuscript. I would also like to thank Middle Eastern Technical University (METU) for the logistical support during the fieldwork. I am very grateful to the personnel of the Kirkit Pension for their hospitality. Thanks are expressed to Maarten Zeylmans Van Emmichoven for the availability and support of the ArcGIS software which enable me to draw the map.

8. REFERENCES

- Atabey, E. 1989. Kayseri - H19 Paftası Jeoloji Haritası. General Directorate of Mineral Research and Exploration (MTA) Publication, Ankara, Turkey.
- Boztug, D., and Jonckheere, R.C., 2007, Apatite fission track data from central Anatolian granitoids (Turkey): Constraints on Neo-Tethyan closure, *Tectonics*, 26, TC3011, doi:10.1029/2006TC001988.
- Boztuğ, D., Jonckheere R.C., Heizler, M., Ratschbacher L., Harlavan Y. and Tichomirova, M., 2009a, Timing of post-obduction granitoids from intrusion through cooling to exhumation in central Anatolia, Turkey, *Tectonophysics* 473, 223–233
- Floyd, P. A., Göncüoğlu, M.C., Winchester, J.A., and Yalnız, M.K., 2000, Geochemical character and tectonic environment of Neotethyan ophiolitic fragments and metabasites in the Central Anatolian Crystalline Complex, Turkey, in *Tectonics and Magmatism in Turkey and the Surrounding Area*, edited by E. Bozkurt, J. A. Winchester, and J. D. A. Piper, *Geol. Soc. Spec. Publ.*, 173, 183 – 202.
- Gautier, P., Bozkurt, E., Hallot, E., Dirik, K., 2002, Dating the exhumation of a metamorphic dome: geological evidence for pre-Eocene unroofing of the Niğde Massif (Central Anatolia), *Geol. Mag.*, vol 139, 559-576
- Gautier, P., Bozkurt, E., Bosse, V., Hallot, E., and Dirik, K., 2008, Coeval extensional shearing and lateral underflow during Late Cretaceous core complex development in the Niğde Massif, Central Anatolia, Turkey, *Tectonics*, 27, TC1003, doi:10.1029/2006TC002089.
- Gökten, E. and Floyd, P.A., 1987, Geochemistry and tectonic environment of the Şarkışla area volcanic rocks in Central Anatolia, Turkey, *Mineralogical Magazine*, 51, 553-559
- Göncüoğlu, M.C, Erler, A., Toprak, G.M.V., Kuşçu, I., 1991, Orta Anadolu Masifin batı bölümünün jeolojisi, Bolum 1: Güney Kesim. T.P.A.O. Report No: 2909, (unpublished)
- Göncüoğlu, M.C, Erler, A., Toprak, G.M.V., Yalnız, K., Kuşçu, I., Köksal, S. and Dirik, K., 1993, Orta Anadolu Masifin batı bölümünün jeolojisi, Bolum 3: Orta Kızılırmak Tersiyer Baseninin jeolojik evrimi, T.P.A.O. Report No: 3313, (unpublished)
- Göncüoğlu, M. C., Dirik, K., and Kozlu, H., 1997, General characteristics of pre-Alpine and Alpine terranes in Turkey: Explanatory notes to the terrane map of Turkey, *Ann. Geol. Pays Helleniques*, 37, 515–536.
- Görür, N., Tüysüz, O. and Şengör, A.M.C., 1998, Tectonic Evolution of the Central Anatolian Basins, *International Geology Review*, 40, 831-850
- Gradstein, F.M., Ogg, J.G., Smith, A., et al., 2004, *A Geologic Time Scale 2004*, 589 pp., Cambridge Univ. Press, New York.
- Gülyüz, E., 2009, Evolution of the Çiçekdağı basin, Central anatolia, Turkey, MSc thesis, Middle East Technical University, Ankara, Turkey (unpublished).
- Van Hinsbergen, D.J.J., and Meulenkamp, J.E., 2006, Neogene supradetachment basin development on Crete (Greece) during exhumation of the South Aegean core complex, *Basin Research*, 18, 103–124, doi: 10.1111/j.1365-2117.2005.00282.x
- Kara, H., and Dönmez, H., 1990, 1:100000 scale geological map of Turkey, Kirsehir-G17 sheet: General Directorate of Mineral Research and Exploration (MTA) no. 34, 17 p. (in Turkish)
- Kaymakci, N., Özçelik, Y., White, S.H. and Van Dijk, P.M., 2009 Tectono-stratigraphy of the Çankırı Basin: Late Cretaceous to early Miocene evolution of the Neotethyan Suture Zone in Turkey, *Geological Society, London, Special Publications*, 311, 67-106, DOI: 10.1144/SP311.3
- Köksal, S. and Göncüoğlu, M.C., 1997, Geology of the Idis Dağı – Avanos Area (Nevşehir – Central Anatolia). *MineralRes. Expl. Bull*, 119, 41-58
- Köksal, S., Göncüoğlu, M.C., Floyd, P.A., 2001, Extrusive members of Postcollisional A-Type Magmatism in Central Anatolia: Karahıdır volcanics, Idis Dağı – Avanos Area, Turkey. *International Geology Review*, 43, 683-694
- Mues-Schumacher, U., and Schumacher, R., 1996, Problems of stratigraphic correlation and new K-Ar data for ignimbrites from Cappadocia, central Turkey: *International Geology Review*, 38, 737–746
- Norman, T.N., Gökçen, S.L., and Şenalp, M., 1980, Sedimentation Pattern in Central Anatolia at the Cretaceous-Tertiary Boundary, *Cretaceous Research*, 1, 61-84
- Okay, A.I., & Tüysüz, O., 1999, Tethyan sutures of northern Turkey, *Geological Society, London, Special Publications*, 156, 475-515, doi:10.1144/GSL.SP.1999.156.01.22
- Okay, A.I., 2008, Geology of Turkey: A Synopsis, *Anschnitt* 21, 19-42.
- Pourteau, A., Candan, O. and Oberhänsli, R., 2010, High-pressure metasediments in central Turkey: Constraints on the Neotethyan closure history, *Tectonics*, 29, TC5004, doi:10.1029/2009TC002650
- Şenel, M., 2002, 1:500000 scale geological map of Turkey, Kayseri sheet: General Directorate of Mineral Research and Exploration (MTA), no 9.
- Şengör, A.M.C. and Yılmaz, Y., 1981, Tethyan evolution of Turkey: a plate tectonic approach, *Tectonophysics*, 75, 181-241.
- Sherlock, S., Kelley, S.P., Inger, S., Harris, N. & Okay ,A.I., 1999, ⁴⁰Ar-³⁹Ar and Rb-Sr geochronology of high-pressure metamorphism and exhumation history of the Tavşanlı Zone, NW Turkey, *Contributions to Mineralogy and Petrology*, 137, 46-58.
- Teklehaimanot, L.T., 1993, Geology and Petrography of Gülşehir Area, Nevşehir, Turkey. MSc thesis, Middle East Technical University, Ankara, Turkey (unpublished).
- Twiss, R.J., and Moores, E.M., 1992, *Structural Geology*, 532 pp, W.H.Freeman and Company, New York.
- Viereck-Goette, L., Lepetit, P., Gürel, A., Ganskow, G., Çopuroğlu, I., and Abratis, M., 2010, Revised volcanostratigraphy of the Upper Miocene to Lower Pliocene Ürgüp Formation, Central Anatolian volcanic

- province, Turkey, in Groppelli, G., and Viereck-Goette, L., eds., *Stratigraphy and Geology of Volcanic Areas: Geological Society of America Special Paper 464*, 85–112
- Wehrens, P.C., 2008, Structural evolution of the Hirkadağ massif, Central Anatolian Crystalline Complex, Turkey, MSc Thesis, Utrecht University, Utrecht, The Netherlands (unpublished).
- Whitney, D.L., Teyssier, C., Dilek, Y., and Fayon, A.K., 2001, Metamorphism of the Central Anatolian Crystalline Complex, Turkey: Influence of orogen-normal collision vs. wrench-dominated tectonics on P-T-t paths, *J. Metamorph. Geol.*, 19, 411 – 432.
- Whitney, D.L., and Dilek, Y., 2001, Metamorphic and Tectonic Evolution of the Hirkadağ Block, Central Anatolian Crystalline Complex, *Turkish Journal of Earth Sciences*, 10, 1-15
- Whitney, D. L., Teyssier, C., Fayon, A.K., Hamilton, M.A. & Heizler, M.J., 2003, Tectonic controls on metamorphism, partial melting, and intrusion: timing of regional metamorphism and magmatism of the Niğde Massif, Turkey, *Tectonophysics*, 376, 37-60.

9. APPENDICES

Appendix 1: Geological map of the Ayhan Basin (scale 1:25000)

Appendix 2: Cross section A (scale 1:25000)

Appendix 3: Cross section B (scale 1:25000)

Appendix 4: Cross section C (scale 1:25000)

**Appendix 1.
Geological Map of the Ayhan Basin**

belonging to:
Advokaat, E.L., 2011,
Tectono-stratigraphic evolution of the Ayhan Basin,
Central Anatolia, Turkey:
A Late Cretaceous to Early Eocene supra-detachment
basin that underwent post-Lutetian compression and
tilting,
MSc Thesis, Utrecht University

Geology of the Ayhan Basin

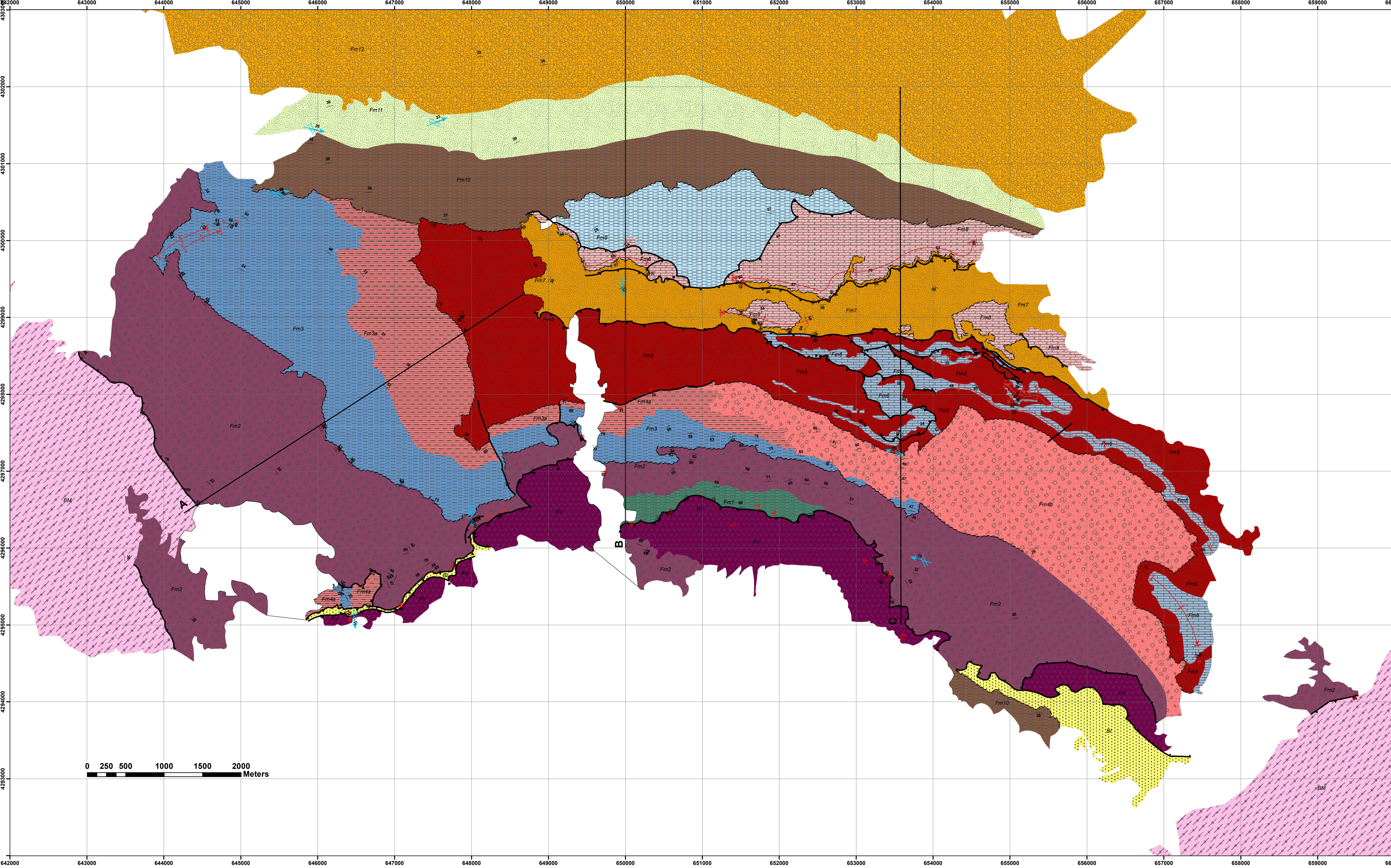
author:
Advokaat, E.L.

geological data:
october 2008

produced:
2010

Projection:
UTM European Datum 1950 Zone 36N

Scale:
1:25000



Key:

	normal beds		Normal fault		Unexposed / Quarternary cover		Fm12: Orange conglomerate		Fm11: Fluvial sands		Fm10: Conglomerate & Lignite bearing Shales <i>lower part: Conglomerate (with metamorphic boulders); upper part: shales, lignite</i>		Fm9: White Marls/Clays		Fm8: Nummulitic Limestone		Fm7: Orange sandstone		Fm6: Lacustrine limestone		Fm5: Dark Red Sandstone
	overturned beds		Thrust fault				Fm4b: Pale Red Conglomerate		Fm4a: Pale Red Sandstone		Fm3: Sandstone member & blue clays		Fm2: Violet conglomerate		Fm1: Black shales		KV: Volcanics		BI: Basement: Intrusive rocks		BM: Basement: Metamorphic rocks
	syncline		Strike-slip fault				<i>conglomerate, sand, silt</i>		<i>sand, silt</i>		<i>lower part: sandstone; upper part: claystone, sandstone</i>		<i>conglomerate (with volcanic boulders), sand</i>		<i>shale, sand</i>		<i>Andesite</i>		<i>Granitoid & Syenitoid</i>		<i>amphibolite, marble</i>
	anticline		Angular Unconformity				<i>clay, marl, sand</i>		<i>Nummulites and oysters present</i>		<i>lower part: shale and clays; upper part: sand</i>		<i>carbonate mudstone</i>		<i>sand, silt</i>						
	Fault plane with dip		Plunging anticline																		
	paleoflow direction		Syncline																		
			Plunging syncline																		

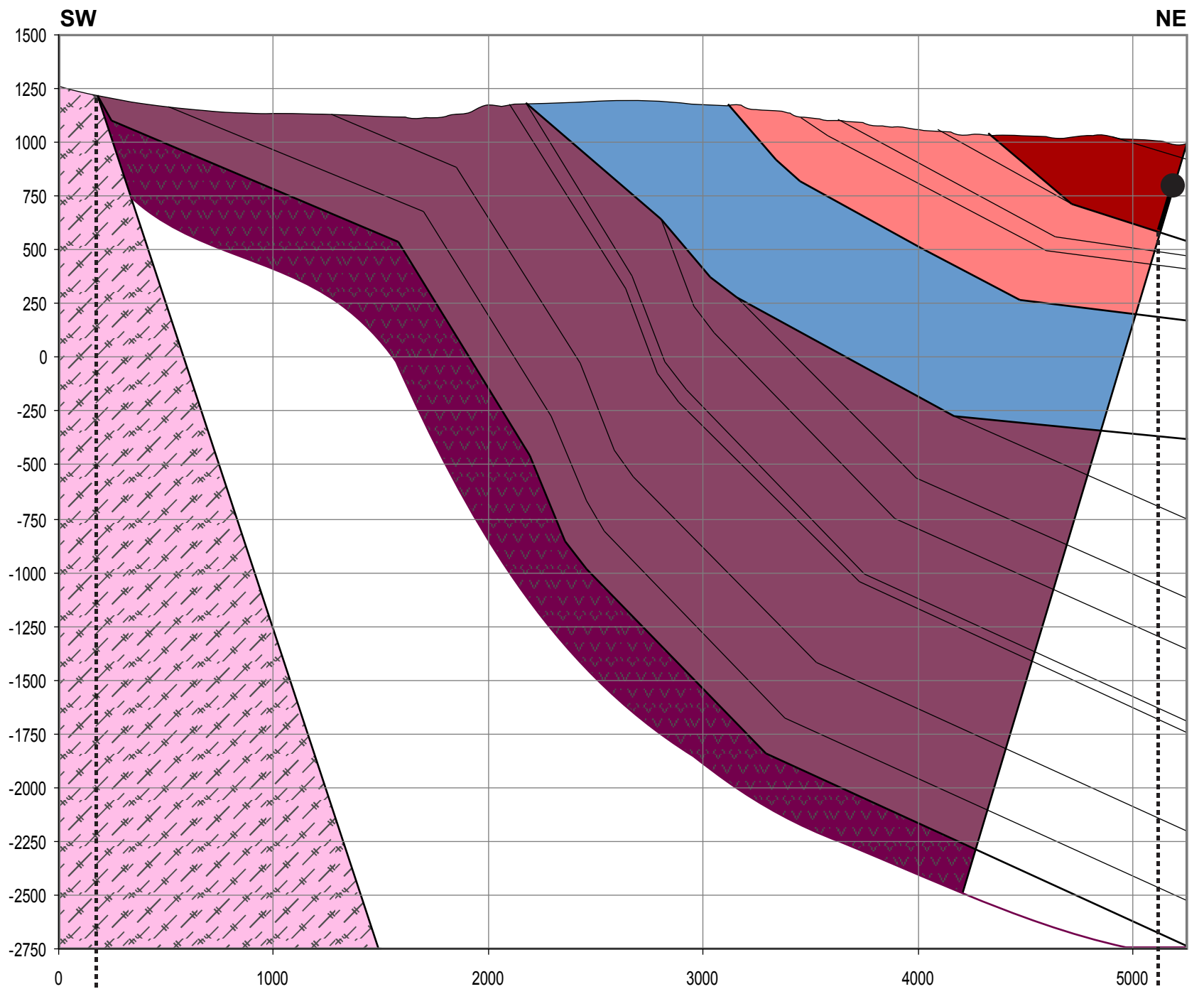


Universiteit Utrecht

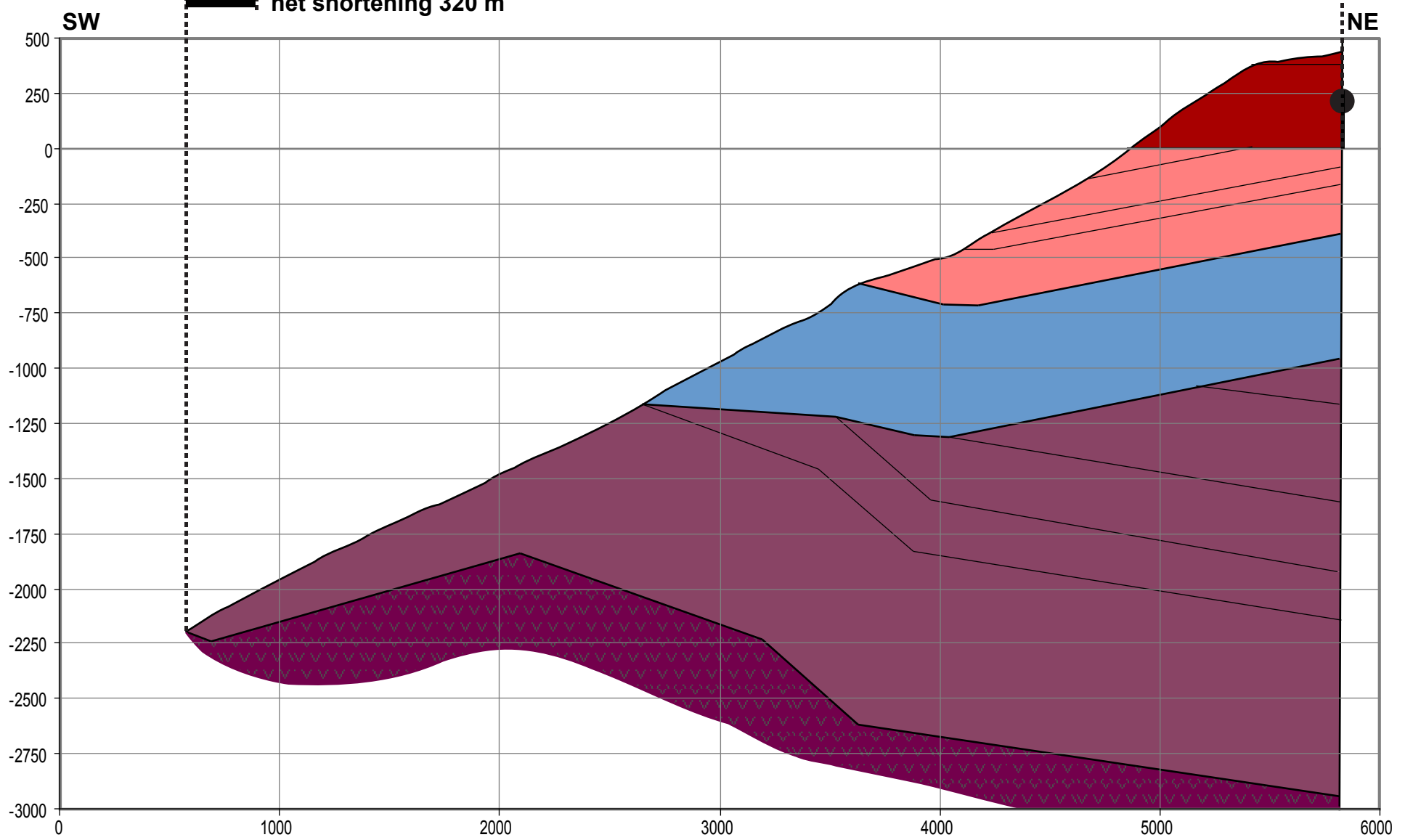


Appendix 2.

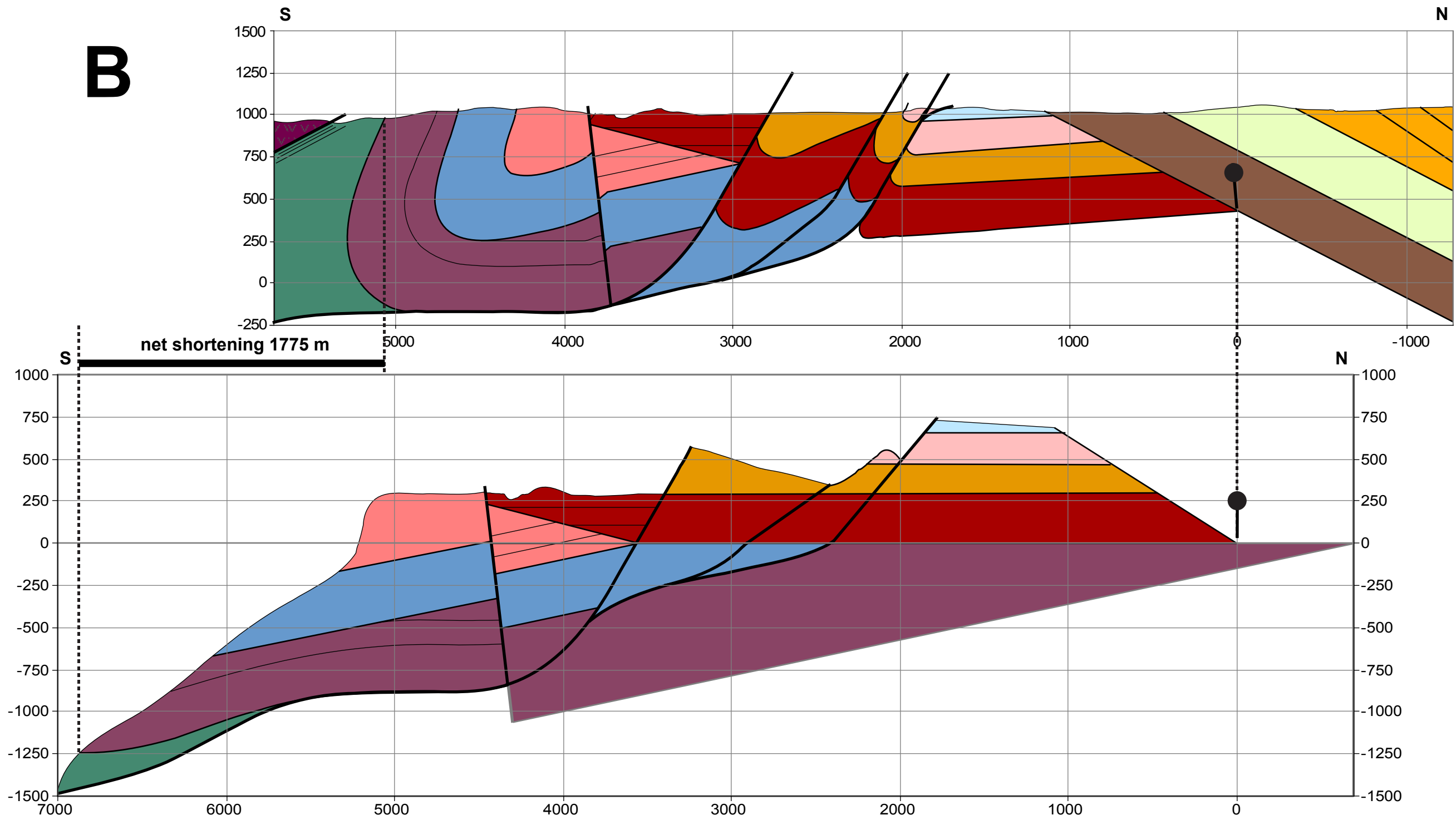
A



net shortening 320 m



Appendix 3.



Appendix 4.

